IEEE Access
Multidisciplinary | Rapid Review | Open Access Journal

SPECIAL SECTION ON COMMUNICATION AND FOG/EDGE COMPUTING TOWARDS INTELLIGENT CONNECTED VEHICLES (ICVS)

Received November 10, 2019, accepted November 22, 2019, date of publication November 26, 2019,
date of current version December 11, 2019.

Digital Object Identifier 10.1109/ACCESS.2019.2955927

Intelligent Vehicle-to-Vehicle Charging Navigation for Mobile Electric Vehicles via VANET-Based Communication

GUANGYU LI[1], QIANG SUN[2], LILA BOUKHATEM[3], JINSONG WU[4], (Senior Member, IEEE), AND JIAN YANG[1]

[1]Key Laboratory of Intelligent Perception and Systems for High-Dimensional Information of Ministry of Education, Nanjing University of Science and Technology, Nanjing 210094, China
[2]School of Mathematical Science, Yangzhou University, Yangzhou 225012, China
[3]Laboratoire de Recherche en Informatique (LRI), University of Paris-Sud, 91405 Orsay, France
[4]Department of Electrical Engineering, University of Chile, 8370451 Santiago, Chile

Corresponding author: Guangyu Li (guangyu.li2017@njust.edu.cn)

This work was supported in part by the Fundamental Research Funds for the Central Universities under Grant 30918014107 and Grant 30919011228, in part by the Natural Science Foundation of Jiangsu under Grant BK20190444 and Grant BK20170480, in part by the National Natural Science Foundation of China under Grant 11801494, and in part by the Fund from Jiangsu Key Laboratory of Image and Video Understanding for Social Safety under Grant KFKT201805.

ABSTRACT A direct vehicle-to-vehicle (V2V) charging scheme supplies flexible and fast energy exchange way for electric vehicles (EVs) without the supports of charging stations. Main technical challenges in cooperative V2V charging may include the efficient charging navigation structure designs with low communication loads and computational complexities, the decision-making intelligence for the selection of stopping locations to operate V2V charging services, and the optimal matching issue between charging EVs and discharging EVs. In this paper, to solve the above problems, we propose an intelligent V2V charging navigation strategy for a large number of mobile EVs. Specifically, by means of a hybrid vehicular ad-hoc networks (VANETs) based communication paradigm, we first study a mobile edge computing (MEC) based semi-centralized charging navigation framework to ensure the reliable communication and efficient charging coordination. Then, based on the derived charging models, we propose an effective local charging navigation scheme to adaptively select the optimal traveling route and appropriate stopping locations for mobile EVs via the designed Q-learning based algorithm. After that, an efficient global charging navigation mechanism is proposed to complete the best charging-discharging EV pair matching based on the constructed weighted bipartite graph. A series of simulation results and theoretical analyses are presented to demonstrate the feasibility and effectiveness of the proposed V2V charging navigation strategy.

INDEX TERMS Electric vehicles, intelligent V2V charging, charging models, VANETs.

NOMENCLATURE

$\Delta\,(e_i)$	Average waiting time for the red traffic light in road segment e_i.
$\omega\,(u.v)$	Weight of edge $e'\,(u, v)$ to evalute the matching performance of charging EV u and discharging EV v.
C	EV battery power capacity.
$CM\,(SL_k)$	Charging comfortable level of an EV in stopping location SL_k.
$EC\,(SL_k)$	Global energy consumption of an EV moving from its current position to the destination going through stopping location SL_k.
$EG\,(u, v)$	Energy gap between demanded energy amount of EV u and supplied energy value of EV v.
$F\,(y)$	Objective function to imply the performance of selected traveling route y.
$G\,(SL_k)$	Feasibility of selected stopping location SL_k.
$L\,(e_i)$	Length of road segment e_i.
N_{ev}^{c}	Number of mobile EVs with V2V charging/discharging concerns.

The associate editor coordinating the review of this manuscript and approving it for publication was Changqing Luo.

N_{mec}	Number of MEC servers.
N_{sl}	Number of stopping locations.
N_v	Number of all moving vehicles including EVs and oil-driven vehicles.
PR_{ev}	Penetration ratio of EVs to all vehicles.
PW	Charging power of EVs.
R	Wireless communication range in VANETs.
T	Information broadcast interval of NCC.
$TA\ (SL_k)$	Arrival time of an EV in stopping location SL_k.
$TC\ (SL_k)$	Charging time of an EV in stopping location SL_k.
$TG\ (u, v)$	Arrival time gap between charging EV u and discharging EV v.
$TR\ (SL_k)$	Global traveling time of an EV moving from its current position to the destination going through stopping location SL_k.
$N_f\ (SL_k)$	Number of free slots in stopping location SL_k in current time.
$T_k\ (e_i)$	Average traveling time of a mobile EV going through road segment e_i.
$T_{cw}\ (SL_k)$	Charging waiting time of EVs for free slots in stopping location SL_k.
$v_k\ (e_i)$	Average traveling velocity of a mobile EV going through road segment e_i.
CC/CV	Constant-current/constant-voltage.
EV	Eletric vehicle
EVC	EVs with charging requirements.
EVD	EVs with discharging abilities.
EVN	EVs without charging/discharging interests.
G2V	Grid-to-vehicle.
IMC	Information managing centers.
ITS	Intelligent transportation systems.
KM	Kuhn-Munkres-based algorithm.
KWh	KiloWatt-hour.
LSTM	Long short-term memory.
MAC	Media access control.
MEC	Mobile edge computing.
MWM	Maximum weighted matching.
NCC	Navigation control center.
OBUs	On board units.
RSUs	Road side units.
SLs	Stopping locations.
SOC	State of charge.
V2G	Vehicle-to-grid.
V2V	Vehicle-to-vehicle.
VANETs	Vehicular ad-hoc networks.

I. INTRODUCTION

With the significantly increasing concerns on the issues of environmental conservations and intelligent transportation systems (ITS), electric vehicles (EVs) have attracted more and more attentions from both industry and academia due to the advantages of zero emissions, low noises, efficient energy conversions and so on [1], [2]. However, the rapid penetration of EVs in traffic scenarios and uncoordinated EV charging operations can result in huge power loss, heavy overloads and serious harmonic distortions [3], all of which are detrimental to the reliability and security of current power systems. To cope with the above challenges, some works [4], [5] have focused on the harmonious charging navigation scheduling for EVs, to efficiently distribute charging loads of EVs and optimize their charging/discharging behaviors on the basis of three main energy exchange operations, namely grid-to-vehicle (G2V), vehicle-to-grid (V2G) and vehicle-to-vehicle (V2V).

In the G2V scheme [6], EVs obtain energy from geographically distributed charging stations to meet the charging demands. In [7], F. Wu et al. introduced a feasible EV charging adaptation model which is formulated as a two-stage stochastic optimization problem, and made use of the Monte Carlo-based sample-average approximation algorithm and L-shaped method to efficiently resolve the mentioned optimization problem, but this fully centralized charging framework would violate privacy of EVs and aggravate wireless network transmission loads due to detailed status information collections of all EVs, result in significantly high computational costs in the case of huge charging/discharging demands of EVs, and may cause severe service interruption once the control center suffers from interferences. The authors [8] presented a distributed charging scheduling algorithm based on the deduced approximation model of waiting time, but this method does not take into account the traveling time and recharging cost in its objective function. In [9], the issue about searching the most available charging station was modeled as a multi-objective optimization problem, which is solved by the proposed ant colony optimization based approach. Nevertheless, the deduced queuing model in this work is not rigorous enough owing to neglecting the charging reservation information of mobile EVs. To decrease the traveling cost of EVs and improve the load level of the concerned distribution system, a dynamic EV charging navigation strategy [10] was proposed based on periodic traffic information update, which can lead to severe congestions in cellular networks and extremely increase communication expense with the dramatic rise of EV number. In [11], the authors designed a mobile edge computing (MEC) based framework for the G2V charging system, where mobility-aware MEC servers (including unmanned aerial vehicles and transportation buses) can keep stable communications with opportunistically encountered EVs, to disseminate CSs' predicted charging availability and collect EVs' driving big data. To achieve efficient inter-connections among aforementioned mobile MEC servers for adequate resource allocations, available air-ground integrated networks with feasible architectures and communication algorithms were proposed in [12], [13].

Through V2G technologies, EVs can act as mobile energy storage facilities and be capable of discharging energy back to power systems to improve energy grid performance [14], [15]. Intensive studies in [16] demonstrated that V2G is

quite effective in alleviating voltage fluctuations and enhancing frequency control of power systems. Ehsani *et al.* [17] validated that V2G can complete protective relay tripping, reduce distribution line losses and mitigate voltage drops. A decentralized V2G management algorithm [18] was proposed to intelligently extract an appropriate amount of energy from EVs for power grid supports during emergent energy conditions, but it would not promise the optimal achievements for coordinated V2G services from the whole system perspectives due to the neglects of global charging information. In [19], a dynamic tariff-subsidy method was designed for congestion managements in distribution networks with the V2G function. Through considering V2G capabilities of EVs, predicted non-EV base loads and so on, the work in [20] established a new adaptive control mechanism to adjust EV charging/discharging behaviors for peak shaving and load balance in power grids. However, EVs participating in V2G operations have to suffer from frequent battery charging/discharging circles, which dramatically increase the internal resistance and reduce the useable capacity of vehicular batteries.

According to the aforementioned descriptions, many EV charging/discharging navigation strategies have been proposed in existing works for both G2V and V2G operations, but these studies have been still restricted to the interactions and energy exchanges between power systems and EVs due to high investments in charging stations and limited charging slots. To cope with the above challenges, some researchers designed a group of more flexible power transferring algorithms on the basis of V2V charging concepts [21], [22], where energy can be exchanged among EVs without charging station supports. Actually, feasible V2V charging is indeed advantageous to both EVs with charging demands and EVs with discharging capacities because of great energy transferring convenience, low energy consumption on traveling to limited charging stations, huge energy trading profits and so on. The work in [23] presented a novel V2V energy trading system with respect to the derived activity-based prediction model, to reduce the negative impacts of the charging process on the power system. In [24], a cloud-based energy transferring structure was designed and an optimal contract-based electricity trading algorithm was proposed to efficiently improve the generated profit. In order to achieve the cooperative V2V charging strategy in dynamic electricity pricing environments, You *et al.* [25] formulated the corresponding charging scheduling problem as a constrained mixed-integer linear program (MILP), which is solved by means of dual decomposition and benders decomposition in a distributed fashion, but this work just focused on EVs having already been parked at charging stations, and neglected the effects of EV mobility on charging coordination [26]. In [27], an online V2V energy swapping strategy (STCC) was proposed based on the feasible price control, which is modeled as an oligopoly game with competitions among EVs, but this work finds EVs' moving routes towards the selected charging locations by means of the shortest-path based algorithm [28], which does not work well in rapidly dynamic traffic environments. In addition, when choosing adequate charging locations for mobile EVs, the proposed algorithm in [27] does not consider the impacts of waiting time in candidate charging locations, which can decrease the comfortable levels of energy exchange for EV drivers and reduce V2V charging efficiency. In fact, the above V2V charging behaviors have to be achieved through the assistance of aggregators, which are responsible for gathering all the information of EVs and grid status, and executing V2V power transferring operations. However, the deployments of aggregators increase the V2V energy exchange costs and reduce the flexibility of V2V charging activities. In addition, most of the above works depend on cellular networks to transmit charging information between EVs and aggregators, but this communication pattern may suffer from high expenses and serious network congestions in the case of a huge number of EVs involving V2V charging activities.

Obviously, it is essential to explore a more flexible and economical V2V charging way to satisfy the increasing charging demands of EVs. Through the aids of bidirectional charging technologies [29] and charging cables connecting EVs, direct V2V charging operations without fixed aggregator demands can be completed in any stopping location (SL) via an approximate charging-discharging EV pair matching scheme, and Fig. 1 shows a simple example about such direct V2V charging services in urban scenarios. To the best of our knowledge, there are very limited studies on direct V2V charging navigation strategies for mobile EVs. In our previous work (DVCS), based on the deduced waiting time model and local traveling energy consumption model, we have proposed a feasible direct V2V charging scheme to minimize charging cost and enhance charging efficiency [30]. However, this algorithm adopts a simple rule of first arrive first service (FAFS) to complete the global matching between charging EVs and

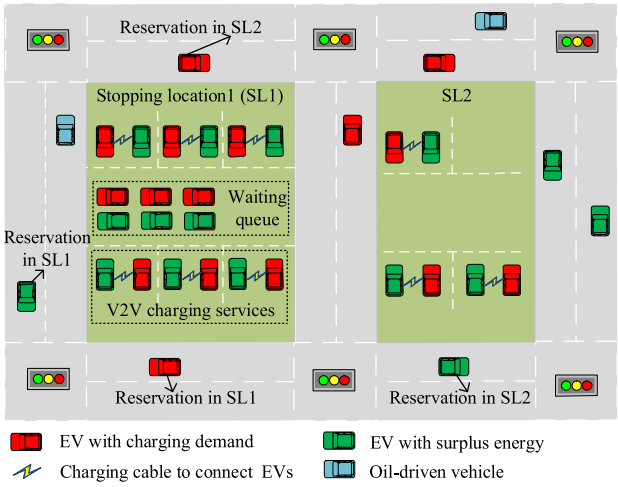

FIGURE 1. A example of direct V2V charging services in urban scenarios, where green EVs with surplus energy are transferring energy to red EVs with charging demands via conductive charging cables.

discharging EVs, and it is not enough to accomplish the optimal EV pair assignments. Note that, In [30], the charging information exchanges between the parking service center and mobile EVs are implemented by more flexible VANETs (vehicular ad-hoc networks) based communications, where all vehicles equipped with OBUs (on board units) can act as data relaying nodes to achieve efficient wireless connections by means of vehicle-to-vehicle and vehicle-to-infrastructure communications [31], [32]. Compared with common cellular networks, VANETs indicate great advantages including low communication expense, no energy constraints, excellent scalability, high self-organization and so forth [33].

In this paper, in order to solve the aforementioned challenges, we propose an intelligent direct V2V charging navigation strategy for a large number of mobile EVs. In particular, to avoid heavy computation loads in traditional centralized manner and achieve the reliable charging information transmission among the navigation control center, distributed stopping locations and moving EVs, we establish a semi-centralized charging navigation framework and design the corresponding management protocol on the basis of flexible VANET-based communication pattern and available mobile edge computing (MEC). In addition, based on the formulated charging models, namely, traveling time prediction model, charging time estimation model and charging comfortable degree model, a feasible local charging navigation scheme is proposed for mobile EVs to adaptively choose the best moving route in varying traffic environments and complete the optimal stopping location selection. Moreover, we develop an effective global charging navigation strategy to assign EVs with charging demands to EVs with additional energy for the optimal charging-discharging EV pair matching.

The main contributions of this work are given as follows.

(1) An efficient charging navigation framework is presented for mobile EVs. Based on the feasible MEC supports, we establish a semi-centralized charging navigation structure by means of more flexible and scalable VANET-based communication, to enable reliable charging information collection and release with low communication expense. Compared with the fully centralized/distributed charging framework, the designed structure can decrease communication congestions and computational costs, enhance EV user privacy, improve scalability and robustness of charging system, alleviate the randomness of EV charging behaviors and achieve V2V charging optimization from global perspectives.

(2) We derive accurate charging models. Based on varying traffic information with time sequences, different charging rate with various battery state of charge (SOC) conditions, busy situations of stopping locations and so on, we deduce three actual charging models including long short-term memory (LSTM) based traveling time prediction model, charging time estimation model and charging comfortable degree model, to achieve efficient V2V charging navigations.

(3) We design an adaptive traveling route selection algorithm. To choose the optimal moving path towards stopping location for subsequent V2V charging services, we propose a Q-learning based optimal method for mobile EVs with charging/discharging demands to sufficiently cope with rapid traffic changes in urban scenarios, by means of predicted traveling time and corresponding energy consumption in each road segment with time series.

(4) We propose an effective global charging navigation scheme. In order to achieve the best charging-discharging EV pair assignment for mobile EVs which have completed the stopping location selections, we formulate the EV pair matching issue as a maximum weighted matching problem based on a constructed bipartite graph with certain weights (where exchanged energy amount, arrival time interval and required energy gap between charging EVs and discharging EVs are taken into account), and propose a feasible optimal algorithm with low complexity, to solve the mentioned problem.

The rest parts of the paper are organized as follows. The system model is depicted in Section II. The proposed effective charging navigation strategy for EVs is illustrated in Section III. Section IV demonstrates the designed strategy performance by means of a series of simulations and analyses. Finally, Section V concludes the paper.

II. SYSTEM MODEL

In this section, we design a MEC-based semi-centralized charging navigation framework and introduce its corresponding management protocol. In addition, we derive three charging models, namely, traveling time prediction model, charging time estimation model and charging comfortable degree model, all of which play significantly important roles in V2V charging coordination processes.

A. SEMI-CENTRALIZED CHARGING NAVIGATION FRAMEWORK

In order to satisfy with the charging/discharging requirements of a large number of mobile EVs in huge-scale urban environments, we propose a feasible and scalable MEC-based semi-centralized charging navigation framework by virtue of hybrid VANET-based communication paradigm, as shown in Fig. 2. The designed charging navigation framework mainly consists of four entities, namely moving EVs, MEC servers, distributed stopping locations (SLs) and navigation control center (NCC).

1) MOVING EVs

According to different vehicular battery SOC levels and traveling energy demands, moving EVs can be divided into three categories including EVs with charging requirements (EVC), EVs with discharging abilities (EVD) (which can be motivated by selling their extra energy to EVC for additional revenue), and normal EVs without charging/discharging interests (EVN). These mobile EVs and other oil-driven vehicles can constitute flexible and scalable VANETs by means of installed on board units (OBUs), to promise the reliable and low-cost transmission between EVs and remote MEC servers via vehicle-to-everything (V2X) communication. Besides,

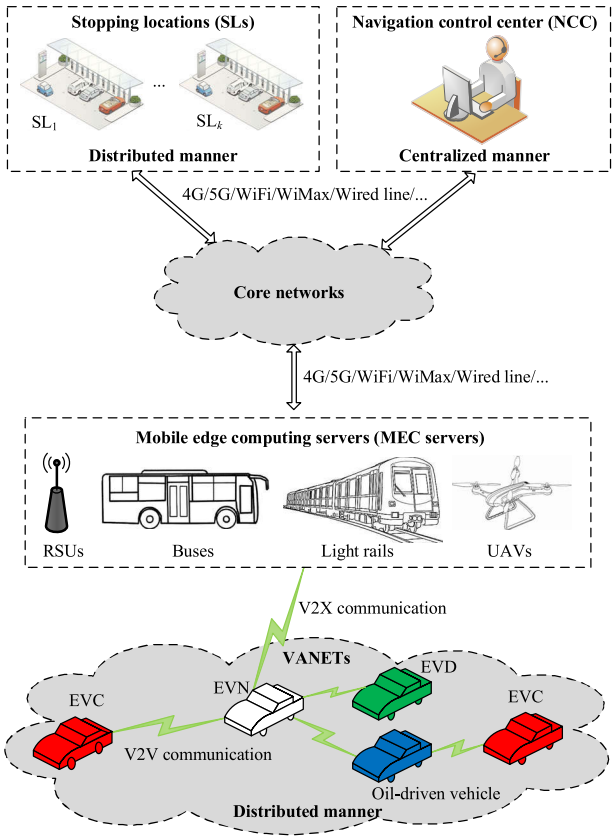

FIGURE 2. Semi-centralized charging navigation framework via VANET-based communication.

based on their own status information (such as current SOC level, moving velocity, current locations and so on) and received charging information (for example, busy situations of stopping locations) from NCC, EVC and EVD are able to perform respective local charging navigation decisions in a distributed manner. Note that, we assume that each EV owns enough space and power to support large vehicular computation resources for local charging navigation tasks.

2) MEC SERVERS

MEC servers can be attached to different communication relaying nodes, such as road side units (RSUs), UAVs, light rails, buses and so forth, and these MEC servers can provide following middle-ware functions to adjacent mobile EVs: (1) operating simple data preprocessing tasks (for example, data cleaning and data aggregation) for gathered charging information from NCC and mobile EVs, to reduce inessential data transmission and ease network congestions, (2) implementing temporary storage for fresh charging information to optimize network performance and improve QoE (quality of experience), and (3) providing data relaying services acting as gateways to effectively alleviate fragile end-to-end connections between NCC and mobile EVs, and to further increase the scalability and feasibility of VANETs in substantial-scale urban scenarios. Obviously, the above MEC servers do not carry out the significantly heavy computation offloading (such as charging navigation decisions) from mobile EVs, and the aforementioned middle-ware functions can be easily achieved on each MEC with low computation time, to improve coordinated V2V charging navigation services, which are regarded as a kind of delay-tolerant application [3]. As a result, it is not very essential to carry out the balance of data preprocessing loads among MEC servers which are required to be inter-connected, to further decrease corresponding execution delay.

3) STOPPING LOCATIONS

SLs are geographically deployed in urban scenarios, and they provide available slots to EVs with charging/discharging demands to implement V2V charging services. In addition, based on the number of occupied slots, the number of EVs waiting for available slots (already arrived in the corresponding stopping location), charging/discharging reservation conditions from mobile EVs and so on, the stopping locations are capable of evaluating their own busy situations in a distributed manner.

4) NAVIGATION CONTROL CENTER

NCC is a logical server established and managed via a cloud computing platform, and it takes charge of collecting and releasing buy situations of all stopping locations, carrying out the global charging navigation operations in a centralized manner, and pushing the final charging decisions to corresponding EVs and SLs to complete V2V charging scheduling and update SLs' busy situations, respectively.

According to the aforementioned descriptions, busy situation estimation of stopping locations and local charging navigation decisions of mobile EVs are implemented in a distributed manner, while global charging navigation decisions are given by NCC in a centralized way, as a result, our proposed MEC-based charging navigation framework is managed in a *semi-centralized* pattern.

B. MANAGEMENT PROTOCOL OF CHARGING NAVIGATION FRAMEWORK

Based on the coordinated V2V charging concept, we propose a conformable management protocol for the designed charging navigation framework. Specifically, when suffering from range anxiety to destinations or owning redundant battery energy, moving EVs can apply for direct V2V energy-swapping services in suitable stopping locations for energy supplements or additional energy exchange revenue. Based on the obtained busy situations of all stopping locations processed by MEC servers, the mobile EVs with charging/discharging demands firstly make local charging navigation decisions to choose the optimal moving route and most appropriate stopping location for further V2V charging operations, and then push the decision messages to NNC going through MEC servers. After that, when receiving the collected local charging navigation decisions, NNC implements global charging navigation operations to realize the

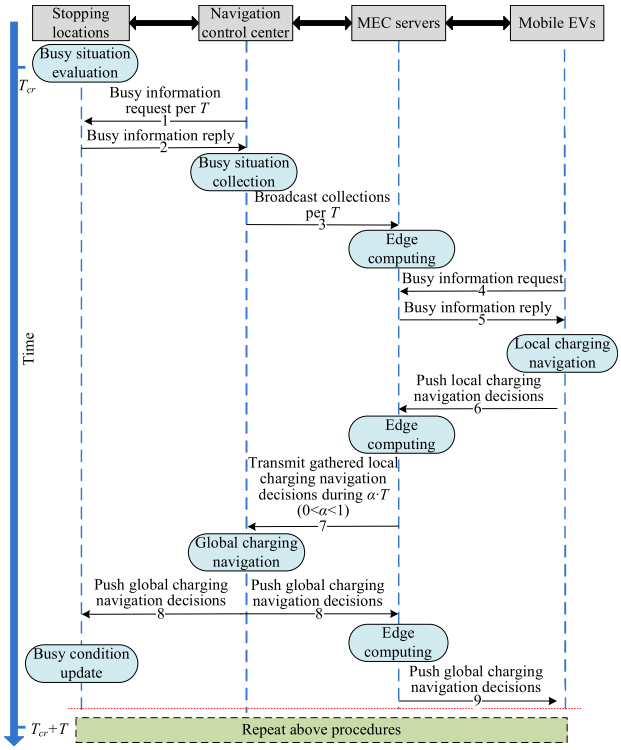

FIGURE 3. Procedure chart of the proposed charging navigation management protocol, where T represents time interval of periodic information dissemination and T_{cr} denotes the current time instant. Besides, we assume that both data preprocessing time T_{dp} and communication delay T_{cd} are much smaller than T ($T_{dp} \ll T$ and $T_{cd} \ll T$).

optimal matching of charging-discharging EV pairs with the same stopping location selection, and then the obtained global decisions are pushed to corresponding EVs and SLs to complete the concerted charging navigation processes. Fig. 3 gives a typical procedure of the designed management protocol, and it is illustrated as follows:

subsectionPROCEDURES 1-3 Operating collection and dissemination of stopping locations' busy situations at NCC side. NCC takes charge of gathering the busy situations of all stopping locations by a reactive communication pattern, and then periodically (time interval T) broadcasts the collected busy information to total MEC servers. Note that, The MEC servers can be capable of the temporal storage and freshness of received busy situations.

1) PROCEDURES 4-6

Carrying out busy situation acquirements and local charging navigation decision deliveries at the sides of mobile EVs. When requiring V2V charing services, mobile EVs firstly request busy situations of all stopping locations from nearby MEC servers by means of established VANETs in a reactive communication way. Then, on the basis of received busy information and their own status conditions (such as current position, velocity, SOC level and so on), mobile EVs implement local charging navigation operations to determine the optimal stopping locations for further V2V charging activities, and then release the local navigation decisions (including the chosen stopping location, arrival time at the selected stopping location and required charging/discharging energy amount) to MEC servers. Note that, the related routing protocols utilized in VANET-based communication are given in our previous works [31], [32], to cope with rapid changes of network topologies and achieve low transmission delay.

2) PROCEDURES 7-9

Implementing global charging navigation calculations and corresponding navigation decision transmission at NCC side. Based on acquired valid local charging navigation decisions (which have been analyzed and mined by MEC servers based on the collected original local navigation decisions of mobile EVs within $a \cdot T$ time interval, and $0 < \alpha < 1$), NCC performs a global charging navigation process for different mobile EVs with the same stopping location selection, to achieve the best charging-discharging EV pair matching appointments. Afterwards, NCC transfers the related global charging navigation decisions to corresponding stopping locations to update their local busy conditions, and to respective MECs, which further relay the processed global information to mobile EVs to satisfy their charging/discharging navigation requirements.

C. CHARGING MODEL DERIVATION

1) TRAVELING TIME PREDICTION MODEL

As an important measurable indicator for the designed smart charging navigation strategy, the traveling time of mobile EVs has closed relationships with segment length, road congestion, traffic light effects and so on. In this paper, we consider that traveling time model of mobile EVs in a road segment is composed of two components including EV's moving time in a selected road segment and waiting time when encountering a red traffic light. In addition, although traffic data (such as vehicle density, moving velocity, etc.) in a road segment presents fast changes with varying time, it still keeps stability in a short time interval. Consequently, we can make use of traffic data with different time series to predict the accurate traveling time in a road segment, and it is derived as:

$$\begin{aligned} T_k(e_i) &= TM_k(e_i) + TW(e_i) \\ &= \frac{L(e_i)}{v_k(e_i)} + \eta(e_i) \cdot p(e_i) \cdot \Delta(e_i) \end{aligned} \tag{1}$$

where $T_k(e_i)$ and $v_k(e_i)$ denote the average traveling time and velocity of a mobile EV going through road segment e_i on the basis of the predicted traffic data in time instant $TI(k) = t + k \cdot \Delta_u$, respectively, where Δ_u represents traffic information update time interval, k is an integer value and $k \geq 0$. $TM_k(e_i)$ and $TW(e_i)$ are the moving time and waiting time during meeting the red traffic light in e_i, respectively, $L(e_i)$ means the length of road segment e_i, $\Delta(e_i)$ implies the average waiting time for the red traffic light in e_i, $\eta(e_i) = \{0, 1\}$ is to indicate whether there is a traffic light located in e_i and 1 implies the traffic light is available, $p(e_i)$ signifies

the probability that an EV suffers from the red traffic light in e_i.

Obviously, $L(e_i)$, $\Delta(e_i)$ and $\eta(e_i)$ can be easily obtained from on-board digital map of mobile EVs, $p(e_i)$ can be assumed as a constant value, while accurately predicting $v_k(e_i)$ is very difficult due to dynamic traffic scenarios. As a result, the derivation of $v_k(e_i)$ is a critical step to establish the feasible traveling time prediction model. In order to realize the above objective, we propose a LSTM-based algorithm to estimate and predict accurate traffic data including traffic flow and traffic density of road segments, to further deduce the effective velocity model.

First of all, the traffic data forecast issue can be transformed into a range of estimation tasks based on time series, and these tasks can be easily solved by LSTM recurrent neural network [34], which enables inside cells to store and read long range contextual information. In each cell of LSTM, based on outputs of its forget gate, input gate and output gate, the cell state is expressed as

$$C_t = F_t \otimes C_{t-1} + I_t \otimes \phi\left(W_c(H_{t-1}, y_t) + b_c\right) \tag{2}$$

and the hidden output is given as

$$H_t = O_t \otimes \phi(C_t) \tag{3}$$

where C_t and H_t denote the state and prediction output of cell at time t, respectively, F_t, I_t, O_t, y_t correspondingly represent the forget gate output, input gate output, output gate output and input of cell at time t, W_c is the weight value, b_c stands for the bias vector, $\phi(\cdot)$ implies the ReLU activation function. The complete cell states and hidden outputs in LSTM can be obtained by means of (2) and (3) recursively with time series.

In addition, LSTM-based prediction model construction and training. To extract deeper and more features of traffic data in high layers, an efficient LSTM-based prediction model is set up and it consists of a input layer with 3-dimensional (3D) tensor, five hidden layers based on LSTM recurrent networks, a flatten layer to compress the return sequences into a 1D tensor, and a fully connected layer (FCL) with *sigmoid* activation. The designed LSTM-based prediction model is presented in Fig. 4. After that, we can input historical traffic data series $\mathbb{X}^*$ into the designed prediction framework to train the LSTM-based recurrent network for complicated traffic data features, where $\mathbb{X}^* = \left\{x^*_{t-m\cdot\Delta_u}, x^*_{t-(m-1)\cdot\Delta_u}, \cdots, x^*_t\right\}$, and the outputs of FCL are the prediction results of traffic data $\mathbb{Z}^* = \left\{x^*_{t+\Delta_u}, x^*_{t+2\cdot\Delta_u}, \cdots, x^*_{t+k\cdot\Delta_u}\right\}$, where $x^*_{t+k\cdot\Delta_u}$ denotes the traffic data set of all road segments in time $t + k\cdot\Delta_u$ and $x^*_{t+k\cdot\Delta_u} = \{Td_k, Tf_k\}$, Td_k and Tf_k mean the traffic density set and traffic flow set in time $t + k\cdot\Delta_u$, respectively.

Finally, according to the traffic flow theory [35], traffic flow, traffic density and moving velocity on a road segment have significant correlations in the spatial-temporal features. Obviously, we can make use of aforementioned predicted traffic data $\mathbb{Z}^*$ to calculate the corresponding average velocity of mobile EVs on a given road segment. The derivation of

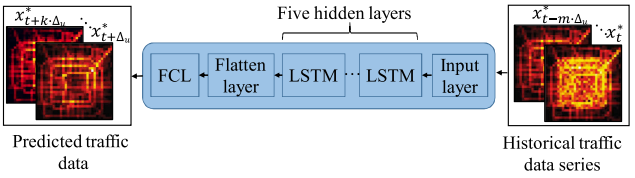

FIGURE 4. LSTM-based prediction model for traffic data forecast.

average velocity is expressed as

$$v_k(e_i) = \frac{Tf_k(e_i)}{Td_k(e_i)} \tag{4}$$

where $Tf_k(e_i)$ and $Td_k(e_i)$ denote the predicted traffic flow and traffic density of road segment e_i in time $t + k\cdot\Delta_u$, respectively, and $Tf_k(e_i) \in Tf_k$, $Td_k(e_i) \in Td_k$.

When substituting (4) into (1), we can complete the traveling time prediction of moving EVs on a given road segment. Note that, the derived traveling time prediction model can be subsequently used to choose the optimal moving route (which consists of a series of road segments) from the current position of an EV to its selected stopping location illustrated in following Section III. Besides, as shown in Fig. 3, after receiving the preprocessed busy information of all stopping locations from MEC servers, mobile EVs with charging/discharging demands begin to implement local charging navigation tasks for the optimal selection of traveling route and stopping location based on the current situation information, such as traveling time, energy consumption and so on. Obviously, offloading time (including data preprocessing time on MEC servers and transmission delay of busy information) from mobile EVs to nearby MEC servers is not relevant to the local charging navigation execution, and it is not essential to be considered in the procedure of traveling time prediction model derivation.

2) CHARGING TIME ESTIMATION MODEL

In order to deduce the charging time model for EVs, we assume that the embedded batteries are lithium-ion battery packs, and a constant-current/constant-voltage (CC/CV) charging strategy is utilized in EV charging process. Specifically, the CC strategy is applied in the first stage of charging procedure, and the battery is recharged until its SOC meets threshold value SOC_{th} with constant power, and the CV scheme is adopted in the following stage, where the gradually-decreasing charging power is used to recharge the battery until its SOC increases from SOC_{th} to 1. The corresponding correlation between the charging power and the charging time is given as follows

$$PW(t_c) = \begin{cases} PW & \text{if } 0 \le t_c \le t_{th} \\ PW \cdot e^{-\sigma(t_c - t_{th})} & \text{if } t_{th} < t_c \le t_f \end{cases} \tag{5}$$

where $PW(t_c)$ indicates the charging power of EV in time t_c, PW means the charging power at CC stage, t_{th} implies the charging time instant when the battery SOC is updated from 0

to SOC_{th}, t_f denotes the time that the battery is fully charged, here $SOC = 1$, and σ is a charging parameter.

Based on the current battery SOC level SOC_c, energy consumption EC towards the selected stopping location (derived in our previous work [30]) and expected exchange energy amount EA, mobile EV can easily predict its charging time, which is estimated by the following equation

$$\int_{t_s}^{t_e} PW\,(t_c)dt = C \cdot (SOC_e - SOC_s) \tag{6}$$

where C is the maximum battery capacity of mobile EV, t_s and t_e represent the charging time interval when the battery SOC value increases from 0 to SOC_s and from 0 to SOC_e, respectively, SOC_e denotes the battery SOC level when EV completes its V2V charging operations, SOC_s indicates the EV's SOC level when it just arrives in the selected stopping location and both of them are derived as follow.

$$\begin{cases} SOC_e = \dfrac{C \cdot SOC_c - EC + EA}{C} \\ SOC_s = SOC_c - \dfrac{EC}{C} \end{cases} \tag{7}$$

According to different values of SOC_e and SOC_s, there are three cases for charging time estimation of EVs by means of (6) and (7).

Case 1: if $SOC_s < SOC_e \leq SOC_{th}$, the whole V2V charging services are implemented via the CC scheme and EV charging time TC is expressed as

$$TC = t_e - t_s = \frac{C \cdot (SOC_e - SOC_s)}{PW} \tag{8}$$

Case 2: if $SOC_s < SOC_{th} < SOC_e$, the battery of EV is recharged by means of the CC and CV charging strategies, and TC is deduced as

$$\begin{aligned} TC =& (t_{th} - t_s) + (t_e - t_{th}) = \frac{C \cdot (SOC_{th} - SOC_s)}{PW} \\ & - \frac{1}{\sigma} \cdot \ln\left(1 - \frac{\sigma \cdot C \cdot (SOC_e - SOC_{th})}{PW}\right) \end{aligned} \tag{9}$$

Case 3: if $SOC_{th} \leq SOC_s < SOC_e$, the complete V2V charging operations of EV are carried out by virtue of the CV charging mechanism, and TC is derived as

$$\begin{aligned} TC &= t_e - t_s \\ &= \frac{1}{\sigma} \cdot \ln\left(\frac{PW - \sigma \cdot C \cdot (SOC_s - SOC_{th})}{PW - \sigma \cdot C \cdot (SOC_e - SOC_{th})}\right) \end{aligned} \tag{10}$$

3) CHARGING COMFORTABLE DEGREE MODEL

We make use of EV waiting time for available stopping slots to subsequently implement V2V charging services and free stopping slot ratio, to evaluate charging comfortable level of EVs in the selected stopping location. Based on the above considerations, the formulated charging comfortable degree model is given as follows.

$$CM\,(SL_k) = \chi \cdot \frac{T_{cw}^{\max} - T_{cw}\,(SL_k)}{T_{cw}^{\max}} + (1-\chi) \cdot \frac{N_f\,(SL_k)}{N^{\max}} \tag{11}$$

where $CM\,(SL_k)$ denotes the charging comfortable level of EV in stopping location SL_k, $T_{cw}\,(SL_k)$ indicates the charging waiting time of EVs for free slots in SL_k, $T_{cw}^{\max}$ means the maximum value among charging waiting time in each candidate stopping location, $N_f\,(SL_k)$ represents the number of free slots in SL_k in current time, N^{max} stands for the maximum value among the total slot number of each stopping location, χ is a weight value and $\chi = \{0, 1\}$, here if $T_{cw}\,(SL_k) = 0$, we set to $\chi = 0$, or $\chi = 1$.

Apparently, if a group of stopping locations with zero waiting time exist, the proposed charging comfortable degree model makes mobile EVs choose the optimal stopping location with the highest free stopping slot ratio, as the selected stopping location owning more available slots can accommodate more EVs to implement V2V energy exchange operations in the same time interval, and the synchronous conflict of stopping location selection can be effectively mitigated. Here the synchronous conflict is defined that a large number of mobile EVs choose the same stopping location in the same time interval for further V2V charging services, as a result, serious congestions in the selected stopping location may occur, and the charging efficiency of EVs can be severely impaired.

So as to complete the above deduction of $CM\,(SL_k)$, it is significantly essential to derive charging waiting time $T_{cw}\,(SL_k)$, which has closed relationships with EVs' arrival time $TA\,(SL_k)$ in SL_k and the earliest free time $TE\,(SL_k)$ of SL_k, here $TE\,(SL_k)$ is defined as the time instant that there are at least two available slots in SL_k for a charging EV and its corresponding discharging EV to operate V2V charging task. As shown in Fig. 1, $TE\,(SL_k)$ can be obtained on the basis of current occupancy situations of slots, waiting queue of parked EV pairs in SL_k and reservation states of mobile EVs for subsequent V2V charging services, charging time and so on, and its detailed derivation is illustrated in our previous work [30]. Note that, the charging time used in $TE\,(SL_k)$ is achieved by our proposed charging time estimation model illustrated in Section. II-C rather than that based on the constant charging rate in [30]. Obviously, if $TE\,(SL_k) \geq TA\,(SL_k)$, all slots in SL_k are fully occupied, and EVs have to await the free stopping space, so $T_{cw}\,(SL_k) = TE\,(SL_k) - TA\,(SL_k)$. When $TE\,(SL_k) < TA\,(SL_k)$, there are available slots for V2V charging services and EVs do not spend extra charging waiting time, so $T_{cw}\,(SL_k) = 0$. According to above illustrations, $T_{cw}\,(SL_k)$ can be derived as follows.

Case 1: if $TE\,(SL_k) \geq TA\,(SL_k)$,

$$T_{cw}\,(SL_k) = TE\,(SL_k) - TA\,(SL_k) \tag{12}$$

Case 2: if $TE\,(SL_k) < TA\,(SL_k)$,

$$T_{cw}\,(SL_k) = 0 \tag{13}$$

Here arrival time $TA\,(SL_k)$ involves current time T_{cu} and traveling time $T_{tr}\left(LC_{ev}, LC_{SL_k}\right)$ from the EV's current location LC_{ev} to its preferred stopping location SL_k, and $T_{tr}\left(LC_{ev}, LC_{SL_k}\right)$ can be calculated by means of the derived traveling time prediction model of road segment in (1) and

the proposed local charging navigation scheme introduced in Section. III-A. $TA\left(SL_k\right)$ is derived as follows.

$$TA\left(SL_k\right) = T_{cu} + T_{tr}\left(LC_{ev}, LC_{SL_k}\right) \tag{14}$$

III. EFFECTIVE CHARGING NAVIGATION STRATEGY

In this section, we propose an efficient charging navigation strategy to achieve feasible coordinated V2V charging services for mobile EVs, and it is composed of both local and global charging navigation schemes.

A. LOCAL CHARGING NAVIGATION SCHEME

In order to decrease heavy communication loads and alleviate serious calculation costs, a distributed local charging navigation algorithm is designed for moving EVs, to choose the most available stopping location for subsequent V2V charging operations based on the proposed dynamic optimal traveling route selection approach.

1) ADAPTIVE OPTIMAL TRAVELING ROUTE SELECTION

To cope with rapidly varying traffic conditions in urban scenarios, a dynamic traveling path selection algorithm with time series is proposed to find the optimal moving route from the EV's current position to its corresponding stopping location with respect to traveling time and energy consumption on this route. In addition, we assume that an urban street map can be abstracted as graph $G\left(E\right)$, where E denotes the road segment set, and we define that candidate traveling route y is composed of a sequence of road segments $\{e_c, \ldots, e_i, \ldots, e_s\}$, where $e_i \in E$, e_c is the road segment in which a mobile EV is moving, and e_s denotes the road segment where the selected stopping location of this EV is located. According to the above considerations, the efficient traveling route selection issue can be formulated as an optimization problem, and the corresponding objective function is expressed as

$$Min\ F\left(y\right) = \lambda_1 \cdot TR\left(y\right) + \lambda_2 \cdot EC\left(y\right) \tag{15}$$

where

$$\begin{cases} TR\left(y\right) = \sum\limits_i T_k\left(e_i\right) \\ EC\left(y\right) = \sum\limits_i EC_k\left(e_i\right) \\ \forall k \in \{0, 1, \cdots, K\} \end{cases} \tag{16}$$

where $F\left(y\right)$ denotes the objective function and it implies the performance of selected traveling route y, $TR\left(y\right)$ and $EC\left(y\right)$ correspondingly mean the traveling time and energy consumption when a mobile EV chooses y, $T_k\left(e_i\right)$ (derived in (1)) and $EC_k\left(e_i\right)$ (deduced in [30]) stand for traveling time and energy consumption when a mobile EV passes through road segment e_i based on the predicted traffic data in time $t + k \cdot \Delta_u$, respectively, λ_1 and λ_2 indicate the weight values.

To solve the above formulated problem, we propose a Q-learning based optimal algorithm, which is skillful in searching the best action-selection strategy even if the agent does not own prior knowledge about its actions' influences on the environment [36]. The concrete procedures of Q-learning based optimal algorithm for traveling route selection are illustrated as follows

Firstly, we regard different road segments in urban scenarios as environment states $S = E = \left\{e_1, \ldots, e_j, \ldots, e_J\right\}$, where J denotes the total number of road segments in urban environment, agent action a is defined as the movement of an EV from one road segment e_j to its neighboring road segment e_l, transfer function $g_s\left(s, a\right)$ denotes the new state to which environment state $s \in S$ changes when agent action a is taken, reward function $g_r\left(s, a\right)$ is given as the received reward after taking action a in state s, where $a \in A$ (A represents the set of agent actions). Here we make use of reward value $g_r\left(s, a\right)$ to show whether the mobile EV arrives in road segment e_s in which the chosen stopping location is located, and $g_r\left(s, a\right)$ is set to 100 if $g_s\left(s, a\right) = e_s$, otherwise, $g_r\left(s, a\right)$ is given as 0. Based on the above description, reward $g_r\left(s, a\right)$ is expressed as follows.

$$g_r\left(s, a\right) = \begin{cases} 100 & \text{if } g_s\left(s, a\right) = e_s \\ 0 & \text{otherwise} \end{cases} \tag{17}$$

Secondly, once entering environment state s, the agent is capable of choosing a feasible action to determine the road segment with better traffic performance. To keep the balance between exploration and exploitation of viable moving route selection, the agent makes use of a simple $\varepsilon - greedy$ method, where ε is a decreasing value with time lapse to make the exploration rate reduce when the agent owns more knowledge about the environments and $0 < \varepsilon < 1$. The $\varepsilon - greedy$ scheme is formulated as follows.

$$P\left(a|s\right) = \begin{cases} 1 - \varepsilon + \dfrac{\varepsilon}{N\left(A\left(s\right)\right)} & \text{if } a = \arg\max\limits_a Q\left(s, a\right) \\ \dfrac{\varepsilon}{N\left(A\left(s\right)\right)} & \text{if } a \neq \arg\max\limits_a Q\left(s, a\right) \end{cases} \tag{18}$$

where $P\left(a|s\right)$ denotes the probability that the agent takes action a when it is in state s, $Q\left(s, a\right)$ indicates a real value with relevant state-action pair and it is used to evaluate the utility performance of action a when the agent is in state s, $A\left(s\right)$ means the set of actions that the agent can take when it is in state s, $N\left(A\left(s\right)\right)$ represents the element number in $A\left(s\right)$ and it also implies the number of neighboring road segments for state s, and $\sum\limits_{l=1}^{N(A(s))} P\left(a_l|s\right) = 1$.

Thirdly, after determining appropriate action a based on current state s, the agent obtains corresponding reward value $g_r\left(s, a\right)$ and its state changes to $s' = g_s\left(s, a\right)$, then the relevant Q value is updated by means of the modified Bellman Equation, which is expressed as follows.

$$Q\left(s, a\right) \leftarrow \left(1 - \partial\right) \cdot Q\left(s, a\right) + \partial \cdot g_r\left(s, a\right) + \gamma \cdot \max_{a'} Q\left(g_s\left(s, a\right), a'\right) \tag{19}$$

where ∂ denotes the learning rate and $0 < \partial < 1$, a' indicates the optimal next action corresponding to next state $g_s\left(s, a\right)$ with the highest Q value, and γ is a discount factor.

In order to adaptively choose the best road segment for mobile EVs and maintain the appropriate effects of both

future and immediate rewards, we devise a piecewise function to dynamically characterize the changes of γ on the basis of traveling time and energy consumption spent on different road segments, and γ is given as follows.

$$\gamma=\begin{cases}\min\left\{\gamma_{\max},\delta\cdot\dfrac{\overline{F}_k(e_l)}{F_k(e_l)}\right\} & \text{if } F_k(e_l)<\overline{F}_k(e_l)\\ \max\left\{\gamma_{\min},\delta\cdot\dfrac{\overline{F}_k(e_l)}{F_k(e_l)}\right\} & \text{otherwise}\end{cases} \tag{20}$$

where $\gamma_{\max}$ and $\gamma_{\min}$ denote the maximum and minimum values of γ, respectively, δ stands for the weight value, $F_k(e_l)$ represents the traffic performance of road segment e_l based on the predicted traffic data in time $t+k\cdot\Delta_u$ (here e_l is a neighbor of current road segment s), and $F_k(e_l)=\lambda_1\cdot T_k(e_l)+\lambda_2\cdot EC(e_l)$, $\overline{F}_k(e_l)$ means the average traffic capability of all neighboring road segments for s, and it is deduced as follows.

$$\overline{F}_k(e_l)=\frac{\sum_{l=1}^{N(A(s))}F_k(e_l)}{N(A(s))} \tag{21}$$

Fourthly, based on the estimated traffic performance of road segments in diverse time and random initial state selection, the agent repeats the aforementioned second and third steps to iteratively choose available actions and update Q values until the final convergence is achieved, which implies that the Q values do not change and corresponding Q-value tables are stable. After a restricted number of iterations, a Q-value table set Q_{tb} for different time slots is obtained to cope with rapid changes of traffic conditions of road segments and $Q_{tb}=\{Q_{tb}(t),Q_{tb}(t+\Delta_u),\ldots,Q_{tb}(t+k\cdot\Delta_u)\}$, where $Q_{tb}(t+k\cdot\Delta_u)$ denotes the stable Q-value table in time $t+k\cdot\Delta_u$.

Finally, based on the pre-stored convergent Q-value tables with various time, mobile EVs can adaptively choose the optimal road segments toward the selected stopping location for V2V charging services, and this dynamic selection procedure is implemented by following the agent actions with the highest Q values. In order to illustrate the basic concept of our proposed optimal route selection strategy, a simple example is given in Fig. 5, in which we define that each road segment e_i stands for a discrete environment state in S, the arrows of solid lines indicate distinct actions moving between neighboring road segments, and the values in close proximity to these solid lines denote the Q values for corresponding actions. In addition, we assume that mobile EV ev_n is moving on e_1 in time t and its selected stopping location is located in e_9. When carrying out the optimal traveling route selection in t, ev_n follows the directions with the highest Q-values to search the best route $R(t)$ towards e_9 based on $Q_{tb}(t)$, and $R(t)=e_1\rightarrow e_2\rightarrow e_5\rightarrow e_8\rightarrow e_9$ marked by red lines in Fig. 5(a). If the predicted position of ev_n along $R(t)$ is located in e_5 in $t+\Delta_u$, a new traveling route selection operation from e_5 to e_9 is launched by means of $Q_{tb}(t+\Delta_u)$ to adapt varying traffic situations, and the selected optimal route $R(t+\Delta_u)$ is $e_5\rightarrow e_6\rightarrow e_9$. The above processes are repeated on the basis of $Q_{tb}(t+j\cdot\Delta_u)$ until the predicted position of ev_n is on e_9. For example, if ev_n can move on e_9 before $t+2\Delta_u$, the optimal traveling route selection process can be completed in time $t+\Delta_u$, and the whole chosen path for ev_n between e_1 and e_9 is determined by combining $R(t)$ and $R(t+\Delta_u)$, and it is given as $e_1\rightarrow e_2\rightarrow e_5\rightarrow e_6\rightarrow e_9$, which is shown by blue lines in Fig. 5(b).

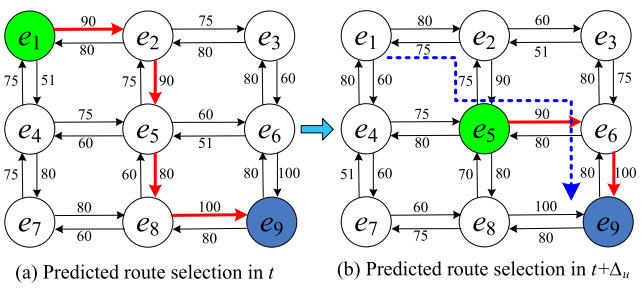

FIGURE 5. An example for the adaptive traveling route selection, where the blue lines indicate the final moving path from road segment e_1 to road segment e_9 for EVs located in e_1 in time t based on Q-value tables with varying time.

2) AVAILABLE STOPPING LOCATION DETERMINATION

In order to cope with the range anxiety and improve the qualities of driving/charging experience of mobile EVs, we consider four factors to evaluate the feasibility of candidate stopping locations for subsequent V2V charging services, namely trajectory-based traveling time, energy consumption, charging time and charging comfortable quality, of which all are derived in Section II-C. In addition, the optimal traveling route for mobile EVs is selected by our proposed algorithm presented in Section III-A rather than a simple shortest-path algorithm. Based on the above discussions, the objective function for available stopping location determination can be formulated as follows.

$$\begin{aligned}\min_{SL_k} G(SL_k)=\lambda_1^s\cdot TR(SL_k)+\lambda_2^s\cdot EC(SL_k)\\ +\lambda_3^s\cdot TC(SL_k)+\lambda_4^s\cdot(1-CM(SL_k))\end{aligned} \tag{22}$$

$$\text{subject to } EC(SL_k)\le C\cdot SOC_c \tag{23}$$

where $G(SL_k)$ denotes the feasibility of selected stopping location SL_k, λ_1^s, λ_2^s, λ_3^s and λ_4^s are weight values, $TR(SL_k)$ and $EC(SL_k)$ indicate the global traveling time and energy consumption of EV moving from its current position to the destination going through SL_k, respectively, $TC(SL_k)$ and $CM(SL_k)$ correspondingly stand for the charging time and charging comfortable degree of EV in SL_k.

So as to solve the formulated function in (22) to complete the available stopping location selection for mobile EVs, we make use of a simple numerical substitution based method due to limited number of stopping locations. In particular, based on the derived models in Section II-C and the optimal traveling route selection scheme in Section III-A, the obtained $EC(SL_k)$ is firstly substituted into (23) to

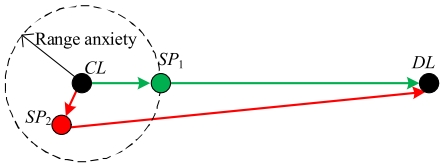

FIGURE 6. An example to validate the effectiveness of global trajectory-based concept.

determine whether it satisfies with the constraint, if yes, corresponding feasible value $G(SL_k)$ is then computed by means of (22). Once all values of $G(SL_k)$ are obtained (where $\forall k \in N$, and N denotes the number of stopping locations in a geographic area), the most available stopping location SL_{op} is easily accomplished and $SL_{op} = \left\{ SL_k \,|\, \min_{SL_k} \{G(SL_k)\}, \forall k \in N \right\}$.

Note that, compared with other researches [27], [30] that only consider local energy consumption $EC(CL, SL_k)$ from EV's current location CL to its selected stopping location SL_k, our trajectory-based factors used in (22) for stopping location selection are more reasonable and make EV drivers undergo lower charging navigation cost from the global trip perspective. An example is depicted to demonstrate such advantages in Fig 6. In the maximum driving range of mobile EV ev_n located in CL, there are two candidate stopping locations (SL_1 and SL_2) for V2V charging services. In the case of local energy consumption concept, ev_n selects SL_2 rather than SL_1 to implement V2V charging operations due to $EC(CL, SL_2) < EC(CL, SL_1)$. However, ev_n has to suffer from higher traveling cost in the future path from SL_2 to its destination location DL compared with that between SL_1 and DL because of $EC(SL_2, DL) \gg EC(SL_1, DL)$. Besides, the computation time of local charging navigation tasks carried out on mobile EVs would make corresponding EVs create redundant movements, which have certain effects on the whole traveling time calculation from the current position of an EV to its selected stopping location, but such computation time is very limited for delay-tolerant V2V charging navigation services and it can be neglected with the purpose to simplify the formulated model. The corresponding reasons are obvious: (1) in the process of adaptive optimal traveling route selection, the states and actions in our proposed Q-learning based optimal algorithm are discrete and their number is limited, which make the corresponding Q-value tables easily converge within the bounded time, (2) based on our designed charging navigation factor models, Q-tables can be calculated via the offline way in advance to further decrease computation time, and (3) in the process of available stopping location determination, the calculation complexity of proposed numerical substitution based method is very low and the number of stopping locations is not large in constructed urban scenarios, both of which achieve the efficient computing task operations with short execution delay.

B. GLOBAL CHARGING NAVIGATION SCHEME

Base on the collected local charging navigation information, as shown in Fig. 3, NNC immediately carries out an efficient global charging navigation scheme to achieve the best charging-discharging pair matching for EVs, which choose the same stopping location for V2V charging services.

From the viewpoint of overall performance of V2V charging system, three targets of our proposed global charging navigation scheme are considered as follows. The first goal is to make EVs exchange as much energy as possible, to sufficiently satisfy with the energy demands of charging EVs and promise high V2V charging revenues of discharging EVs. In addition, the sum of arrival time interval between charging EV and discharging EV assigned in one matching pair should be minimized to decrease extra waiting time for further V2V energy exchanges. The final objective is to minimize the total gaps between demanded energy from charging EVs and supplied energy from discharging EVs, so as to efficiently balance the supply and demand requirements of different EVs, and defend the benefits of discharging EVs as much as possible. To effectively achieve the aforementioned targets, we regard the charging-discharging EV pair matching issue as a maximum weighted matching (MWM) problem based on a designed bipartite graph $G = (U, V, E')$ with weight $\omega : E' \rightarrow \mathbb{R}$, where U and V represent charging EV set and discharging EV set with the same stopping location selection, respectively, E' means the edge set implying the candidate matching between U and V. According to the above descriptions, the introduced charging-discharging pair matching problem can be formulated as follows.

$$\max \; P = \sum_{\forall u \in U} p_u \tag{24}$$

$$\text{subject to} \begin{cases} p_u = \sum_{\forall v \in V} \omega(u, v) < 2, & \forall u \in U \\ \sum_{\forall u \in U} \omega(u, v) < 2, & \forall v \in V \end{cases} \tag{25}$$

where $\omega(u, v)$ denotes the weight of edge $e'(u, v) \in E'$, and it is used to evaluate the matching performance of charging EV u and discharging EV v.

In order to achieve the mentioned objectives of global charging navigation, we induce $\omega(u, v)$ in terms of three parameters, namely exchanged energy amount, arrival time interval and required energy gap between u and v, and two cases are considered as follows.

Case 1: if demanded energy amount EY_u^d of u is no more than supplied energy value EY_v^s of v, and arrival time interval $TG(u, v)$ between u and v does not exceed configured maximum value TG, that is $\left(EY_u^d \le EY_v^s\right) \cap (TG(u, v) \le TG)$, the matching between u and v is feasible, and $\omega(u, v)$ is derived as

$$\omega(u, v) = 1 + \alpha_1 \cdot \frac{EY_u^d}{C} + \alpha_2 \cdot \frac{TG - TG(u, v)}{TG} + \alpha_3 \cdot \frac{EG_{\max} - EG(u, v)}{EG_{\max} - EG_{\min}} \tag{26}$$

Case 2: if $\left(EY_u^d > EY_v^s\right) \cup (TG(u,v) > TG)$, the matching between u and v is not effective, and $\omega(u,v)$ is given as

$$\omega(u,v) = 0 \tag{27}$$

where $TG(u,v) = |TA_u - TA_v|$, TA_u and TA_v mean the arrival time in the selected stopping location of u and v, respectively, C is the maximum battery capacity, $EG(u,v) = EY_v^s - EY_u^d$, $EG_{\max} = \max\{EG(u,v)|\forall u \in U, \forall v \in V\}$, $EG_{\min} = \min\{EG(u,v)|\forall u \in U, \forall v \in V\}$, α_1, α_2 and α_3 are weight factors and all of them are more than 0, and $\alpha_1 + \alpha_2 + \alpha_3 = 1$.

According to the above descriptions, (25) can ensure that each charging EV in U is capable of being put into one-to-one correspondence with each discharging EV in V. Besides, C_u, TG, $EG_{\max}$ and $EG_{\min}$ in (26) are utilized to remove the dimensional characteristic effects of different matching performance parameters in the normalization process.

To solve the above formulated MWM problem in (24) with constraints expressed as (25), we propose an efficient *Kuhn-Munkres* (KM) [37] based algorithm. Specifically, we start with an initial matching M and a valid labeling y, where y is defined as the labeling $\{y(u) \leftarrow \max_{v \in V} \omega(u,v), y(v) \leftarrow 0 | \forall u \in U, \forall v \in V\}$. After that, we search a candidate augmenting path starting at vertex u to extend M, where $u \in U$, $u \notin M$. If a feasible augmenting path exists, the matching is updated via replacing the edges in M with the edges in the augmenting path that are not in M. In the case that there is not a feasible augmenting path, we carry out labeling improvement operations to form an extended subgraph and then go back to the step of candidate augmenting path search for tight edges. The above procedures are constantly implemented until a maximum matching is found. In the process of labeling improvement, we firstly let ψ be the minimum of $y(u) + y(v) - \omega(u,v)$ over all of $u \in U'$ and $v \in V/V'$ (which is defined as $v \in V$ and $v \notin V'$), and then based on the deduced ψ, labeling y is improved by means of the following expression.

$$y(x) \leftarrow \begin{cases} y(x) - \psi & \text{if } x \in U' \\ y(x) + \psi & \text{if } x \in V' \end{cases} \tag{28}$$

where U' and V' are reachable vertex sets in the explored augmenting alternating path, and $U' \subseteq U$, $V' \subseteq V$.

The detailed steps of proposed KM-based optimal matching algorithm is given in Algorithm 1, and a simple example to illustrate the best charging-discharging EV pair assignment is presented in Fig. 7, in which there are three charging EVs and four discharging EVs, and the weight values of different matching pairs via (26) and (27) are indicated next to the corresponding solid lines. After several iterations based on our proposed KM-based matching algorithm, the optimal EV matching results are given, that is u_1 to v_4, u_2 to v_3 and u_3 to v_1, all of which are represented by black bold line, red bold line and green bold line, respectively.

Algorithm 1 An Efficient KM-Based Matching Algorithm for the Optimal Charging-Discharging EV Pair Assignments

1: $y(u)$: the label of u.
2: $y(v)$: the label of v.
****
3: $y(u) \leftarrow \max_{v \in V} \omega(u,v), \forall u \in U$.
4: $y(v) \leftarrow 0, \forall v \in V$.
5: $E_t' \leftarrow$ Set of explored tight edge $e'(u,v)$, where $y(u) + y(v) = \omega(u,v)$.
6: $M \leftarrow$ Maximum cardinality matching for graph $G' = \left(U, V, E_t'\right)$.
7: **while** M is not a maximum matching **do**
8: Explore an augmenting path for M starting from an appointed unmatched vertex in U.
9: **if** no augmenting path exists **then**
10: $U' \leftarrow \{u' | u'$ is a reachable vertex in the explored augmenting alternating path, $u' \in U\}$.
11: $V' \leftarrow \{v' | v'$ is a reachable vertex in the explored augmenting alternating path, $v' \in V\}$.
12: $\psi = \min\left\{y(u) + y(v) - \omega(u,v) | u \in U', v \in V/V'\right\}$.
13: $y(u) \leftarrow y(u) - \psi, \forall u \in U'$.
14: $y(v) \leftarrow y(v) + \psi, \forall v \in V'$.
15: New edge $e'(u_c, v_c)$ is added to extend the existing tight subgraph, where $\{u_c, v_c\} \leftarrow \arg\min_{u,v} \psi(u,v)$.
16: Go back to line 8.
17: **end if**
18: Update E_t' and M.
19: **end while**
20: Return M.

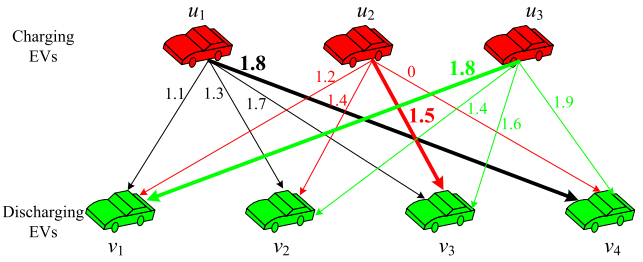

FIGURE 7. The optimal charging-discharging EV pair matching example by means of KM-based algorithm. The best assignment results are given as follows: u_1 matches with v_4, u_2 matches with v_3, u_3 matches with v_1.

IV. PERFORMANCE AND DISCUSSIONS

In this section, we evaluate the performance of proposed Intelligent Direct V2V Charging Navigation strategy (IDCN). In addition, to better illustrate the advantages of our designed IDCN scheme, five efficient charging navigation strategies are utilized as the benchmarks including STCC [27], DVCS [30], GCNA (greedy charging navigation algorithm, where the nearest stopping location is selected for V2V charging service, and matching pairs are assigned as long

TABLE 1. Simulation parameters.

Parameter	Value
Urban scenario size	4 km × 3.7 km
EV battery capacity C	85 KWh
Charging power PW	17.2 KW
Initial remaining energy of each EV	$15-80$ KWh
Charging/discharging energy amount	$10-30$ KWh
Penetration ratio of EVs to all vehicles PR_{ev}	$10\%-20\%$
Maximum charging waiting time T_{cw}^{max}	4 h
Traffic information predicted interval Δ_u	0.25 h
Maximum value of discount factor $\gamma_{\max}$	0.85
Minimum value of discount factor $\gamma_{\min}$	0.25
Maximum arrival time gap TG	0.5 h
Weight value δ	0.6
Weight values α_1,α_2 and α_3	$\frac{1}{3}$, $\frac{1}{3}$, $\frac{1}{3}$
Communication range in VANET R	200 m, 250 m
Wireless transmission capacity	6 Mbps
MAC layer protocol	802.11p

as the demanded energy of charging EVs is less than the corresponding supplied energy of discharging EVs), IDCN_S (a defined version of IDCN where the optimal traveling route for mobile EVs is determined based on the static Q-value table at the current time rather than the varying Q-value tables with different time, and V2V charging reservation situations are not considered in the derived charging comfortable degree model) and ACMS, where the charging navigation scheme is almost same as that of our proposed IDCN, except that both local and global charging navigation missions are implemented on MEC servers rather than on distributed EVs and centralized NCC in IDCN, respectively.

A. EXPERIMENTAL ENVIRONMENTS

To implement our experiments, a realistic urban scenario extracted from Nanjing city, Jiangsu province, China, is considered in the simulations, and its area size is set to 4 kilometers (km) × 3.7 km, as shown in Fig. 8, and practical traffic dataset of mobile vehicles moving on the above region is given by Nanjing Transport Bureau from January 1 to April 5, 2018. In addition, we assume that the type of mobile EVs is TESLA Model S, and EV battery capacity C and charging power PW are set to 85 KiloWatt-hour (KWh) and 17.2 KiloWatts (KW), respectively, initial state of remaining energy in the battery for each EV is uniformly selected from [15, 80] KWh, and the penetration level of EVs is give as $10\%-20\%$. Moreover, we consider that maximum charging waiting time T_{cw}^{max} is given as 4 hours (h), traffic information predicted interval Δ_u is 0.25 h, maximum value $\gamma_{\max}$ and minimum value $\gamma_{\min}$ of discount factor are presented as 0.85 and 0.25, respectively, and maximum arrival time gap TG is set as 0.5 h. Furthermore, δ is set as 0.6, α_1, α_2 and α_3 are given as $\frac{1}{3}$, respectively. Finally, in VANET-based communication scenarios, wireless communication range of vehicles is fixed to 200 and 250 meters (m), channel transmission capacity is set to 6 Million bits per second (Mbps), and the media access control (MAC) layer protocol is given as 802.11p. The detailed simulation parameters are described in table. 1.

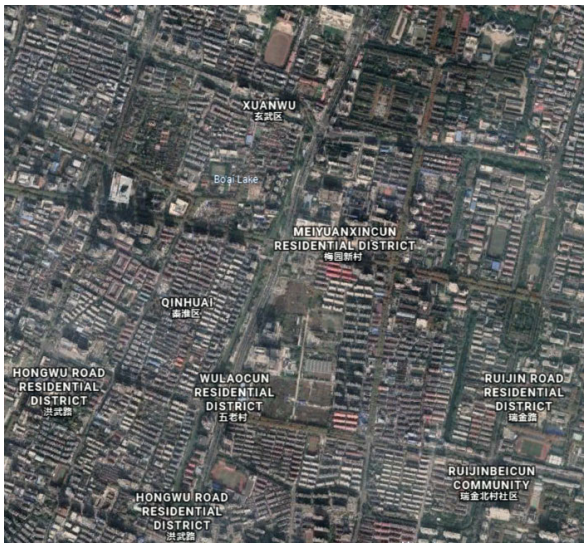

FIGURE 8. A snapshot of the realistic simulation scenario.

B. COMMUNICATION PERFORMANCE EVALUATION

1) THEORETICAL ANALYSIS ON TRANSMISSION COST

We define the transmission cost as the total number of established delivery connections during communication period. Compared with the number of other entities of charging navigation framework, such as stopping locations, mobile EVs, MEC servers, the amount of information managing centers (IMC, which is renamed as navigation control center in IDCN, parking service center in DVCS, and aggregator in STCC) is very limited, as a result, an IMC can be regarded as the communication bottleneck of the overall charging navigation framework, and it easily suffers from the passive effects of big V2V charging information delivery. Obviously, it is very critical to analyze the transmission cost of each IMC for various charging navigation strategies. As the IMC communicates with stopping locations and MEC servers for local/global charging navigation messages in each $\alpha \cdot T$ period ($0 < \alpha < 1$), as shown in Fig. 3, the transmission cost in proposed IDCN is scaled by $\Theta\left(\frac{N_{sl}+N_{mec}}{\alpha \cdot T}\right)$, where N_{sl} and N_{mec} denote the number of stopping locations and MEC servers, respectively, T means the broadcast time interval. In addition, every IMC in STCC collects real-time charging/discharging profiles from mobile EVs with V2V charging/discharging requirements, and broadcast the calculated price decisions to all mobile vehicles per T, so the transmission cost of IMC is given as $\Theta\left(N_{ev}^{c}+\frac{N_v}{T}\right)$, where N_{ev}^{c} indicates the number of mobile EVs with V2V charging/discharging concerns, and N_v is the number of all moving vehicles including EVs and oil-driven vehicles. Moreover, IMC suffers from the transmission cost of $\Theta\left(N_{sl}+N_{ev}^{c}+\frac{N_v}{T}\right)$ in DVCS, since it broadcasts busy situations of all stopping locations to mobile vehicles per T, and gathers (pushes) real-time V2V charging information from (to) both stopping locations and moving EVs with V2V

TABLE 2. Transmission cost of charging navigation.

Charging navigation strategy	Transmission cost
STCC	$\Theta\left(N_{ev}^{c}+\frac{N_v}{T}\right)$
DVCS	$\Theta\left(N_{sl}+N_{ev}^{c}+\frac{N_v}{T}\right)$
IDCN	$\Theta\left(\frac{N_{sl}+N_{mec}}{\alpha\cdot T}\right)$

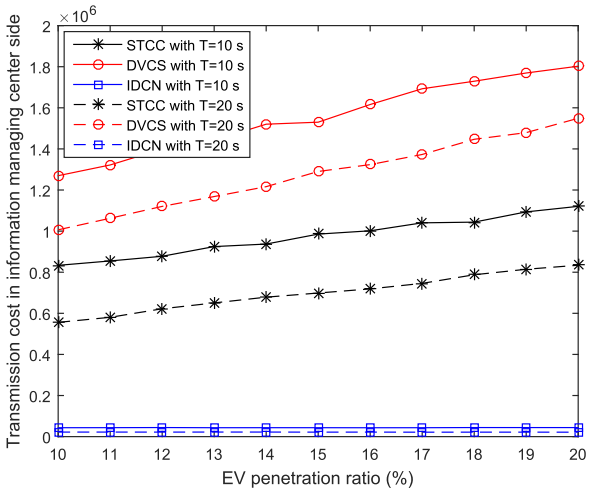

FIGURE 9. Transmission cost with different EV penetration ratio and broadcast time intervals.

charging/discharging requirements, to complete the feasible charging navigation tasks. The transmission costs of three different charging navigation strategies are summarized in table 2. Obviously, based on the general knowledge, $N_{mec} \ll N_{ev}^{c}, N_{sl} \ll N_v$, and thus the transmission cost of our proposed IDCN is much lower than that of STCC and DVCS. Besides, table 2 shows that the transmission cost in IDCN is only proportional to the number of MEC servers and stopping locations rather than the larger number of moving vehicles, as a result, IDCN presents highly significant scalability compared with other charging navigation strategies.

2) EXPERIMENTAL VALIDATION ON TRANSMISSION COST

Fig. 9 shows the transmission cost of each IMC in different charging navigation strategies with varying EV penetration ratio and broadcast time interval T. From this figure, we see that transmission costs of all charging navigation strategies increase with the decrease of broadcast time interval T, which leads to raise communication frequency and establish more transmission connections. In addition, we observe that the transmission cost in both STCC and DVCS is directly proportional to the EV penetration ratio levels, as higher EV penetration ratio implies more EVs requiring V2V charging services, which can result in more substantial communication demands. Furthermore, the transmission cost in the proposed IDCN keeps stability with varying EV penetration ratio and it indicates the lowest values compared with those of other charging navigation strategies, so IDCN owns better performance in the aspects of big

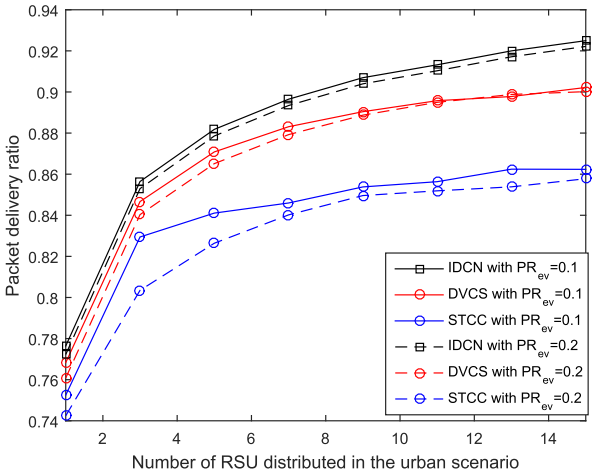

FIGURE 10. Packet delivery ratio with different RSU number and EV penetration ratio.

data transmission and network congestion alleviation. Apparently, Fig. 9 exhibits the communication effectiveness of our established MEC-based semi-centralized charging navigation framework, and the above simulation results are in accordance with the theoretical analysis in Section IV-B-1.

3) PACKET DELIVERY RATIO EVALUATION

Fig. 10 displays the end-to-end packet delivery ratio between IMC and mobile EVs based on varying EV penetration ratio and different number of RSUs, which are uniformly distributed in urban scenarios. From this figure, we observe that the proposed IDCN indicates the highest packet delivery ratio compared with other referencing schemes, because each RSU in IDCN owns MEC capacities and it can carry out data mining and aggregation operations to remove unqualified charging information, which is advantageous to communication congestion alleviation and transmission interference reduction. In addition, more RSUs are capable of dividing the enormous urban environment into several smaller local areas, and charging information can arrive in its IMC by passing through shorter wireless distance, which implies less effects from communication channel fading, noise interferences and so on, so packet delivery ratio can be further enhanced. Moreover, Fig. 10 shows that packet delivery ratio slightly decreases with the rise of EV penetration ratio, and the reason is obvious: higher EV penetration ratio implies that V2V charging/discharging demands increase, and more charging information should be exchanged between mobile EVs and IMC, as a result, serious communication congestions may occur and packet delivery losses may rise.

4) AVERAGE OFFLOADING TIME

As presented in Fig. 11, the average offloading time from EVs to nearby MEC servers is evaluated with respect to various EV penetration ratio and communication ranges in VANETs, here we define that offloading time is composed of two parts including data processing time on MEC servers

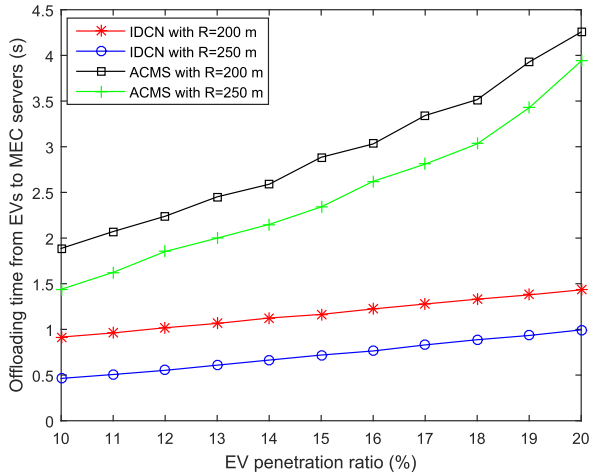

FIGURE 11. Offloading time with different EV penetration ratio and communication range.

and transmission delay between MEC servers and EVs. From this figure, we observe that offloading time in our proposed IDCN is below 1.5 seconds, and it is very low compared with the whole traveling time of EVs towards the selected stopping locations. Two reasons are given to explain such results. Firstly, the available communications between mobile EVs and adjacent MEC servers are carried out by means of efficient VANETs, where our proposed adaptive routing protocols [31], [32] are implemented to achieve low transmission delay. Secondly, the data preprocessing tasks on each MEC server are very simple, and corresponding computation time is indeed short. In addition, from Fig. 11, we see that the offloading time of ACMS is significantly higher than that of IDCN, and such results can be explained as follows: (1) MEC servers of ACMS would gather more exhaustive charging information from mobile EVs and more data would pour into VANETs connecting MEC servers and mobile EVs, so severe network congestions may occur and transmission delay increases, and (2) both preprocessing tasks for more charging information and charging navigation missions would be operated on MEC servers of ACMS, and corresponding computation time substantially increases especially in the case of high EV penetration ratio. Moreover, Fig. 11 indicates that offloading time decreases with the rise of communication range, which makes broken wireless links in VANETs be recovered and the corresponding delivery delay is reduced.

C. CHARGING NAVIGATION PERFORMANCE EVALUATION

1) DETOURING CHARGING NAVIGATION COST

Table 3 presents the detouring charging navigation cost of different algorithms, namely detouring traveling time and detouring energy consumption. Here detouring traveling time is defined as the difference between traveling time of an EV's current trip $R(CL, DL, SL)$ from its current location CL to destination DL passing through selected stopping location SL and that of the direct trip $R(CL, DL)$ from CL to DL, and

TABLE 3. Detouring traveling time and energy consumption for each mobile EV.

		IDCN	IDCN_S	DVCS	STCC	GCNA
Detouring traveling time (unit: s)	Maximum	91.11	97.38	110.64	109.01	110.94
	Minimum	88.19	89.58	100.62	99.19	89.01
	Median	89.59	94.41	104.23	104.41	101.13
	Mean	89.71	94.19	104.52	104.12	101.21
	Std.	0.75	1.88	2.48	2.11	3.83
Detouring energy consumption (unit: KWh)	Maximum	0.39	0.52	0.78	0.74	0.88
	Minimum	0.23	0.14	0.10	0.08	0.13
	Median	0.32	0.37	0.42	0.42	0.47
	Mean	0.32	0.37	0.44	0.43	0.46
	Std.	0.03	0.08	0.14	0.14	0.15

detouring energy consumption is given as the gap between traveling energy consumption of $R(CL, DL, SL)$ and that of $R(CL, DL)$. In addition, in this experiment, we set the number of stopping locations and EV penetration level to 5 and 20%, respectively. From this table, we observe that the proposed IDCN algorithm indicates the best charging navigation performance compared with other strategies in terms of mean values and standard deviations (std.) of detouring traveling time and detouring energy consumption, respectively. The reasons are given as follows: (1) when selecting available stopping locations for V2V charging services, IDCN takes into account both *global trajectory-based* traveling time and energy consumption of $R(CL, DL, SL)$ rather than local performance of route from CL to SL in other referencing algorithms (GCNA, STCC and DVCS), and the extra charging navigation cost can decrease as much as possible, and (2) when determining the moving route for mobile EVs, IDCN is capable of dynamically selecting the optimal traveling path based on predicted traveling time and energy consumption of road segments in varying time series, while both the shortest-path algorithm (used in GCNA, STCC and DVCS) and the static route selecting scheme (applied in IDCN_S) can not effectively cope with the rapid changes of traffic conditions, and they may lead to higher charging navigation cost.

2) AVERAGE WAITING TIME FOR CHARGING SERVICES

Fig. 12 shows the relationships among average waiting time of each EV, EV penetration ratio PR_{ev} and stopping location number N_{sl} for different charging navigation schemes. It is observed that the waiting time of all charging navigation strategies increases with ascending EV penetration ratio, which implies more EVs with charging requirements, and the existing stopping slots are not enough for huge V2V charging demands. In addition, this figure displays that higher stopping location number is beneficial to the decrease of EVs' waiting time, as more stopping locations can provide mobile EVs with more feasible energy exchange sites, which are advantageous to improving charging efficiency and reducing average waiting time. Moreover, from Fig. 12, we can see that the waiting time of IDCN, IDCN_S and DVCS is lower than that of STCC and GCNA, because the influences of waiting time are considered in these three algorithms (IDCN,

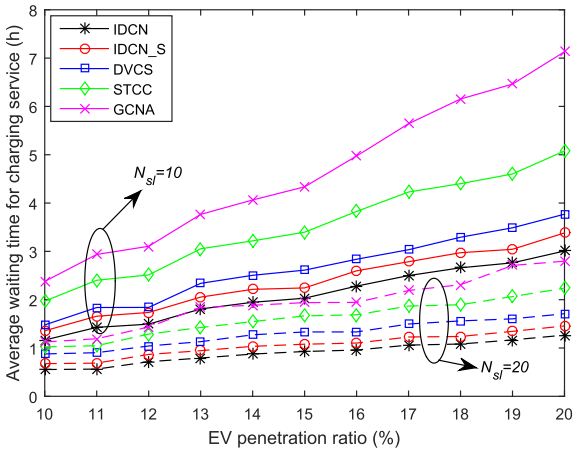

FIGURE 12. Waiting time with different EV penetration ratio and stopping location number.

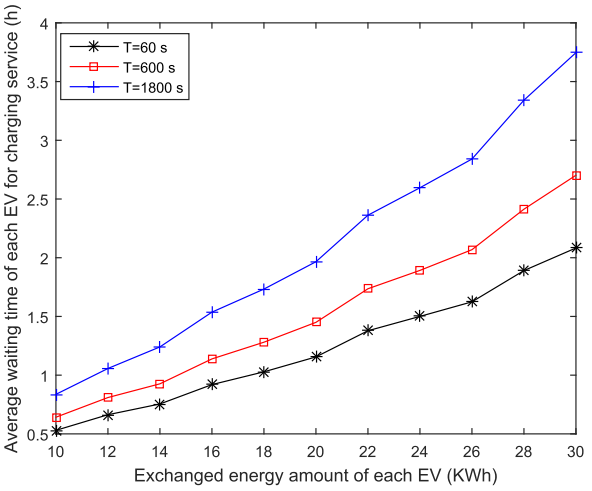

FIGURE 13. Waiting time with different exchanged energy amount and broadcast time intervals.

IDCN_S and DVCS) when they select the available stopping location. Furthermore, as described in Fig. 12, the proposed IDCN charging navigation algorithm achieves the lowest waiting time compared with that of other strategies, and such results can be explained as follows. Firstly, IDCN makes use of Q-learning based method to adaptively choose the optimal traveling route, as a result, we can estimate more accurate arrival time, which could be conducive to choosing the stopping location with better charging comfortable degree and decreasing waiting time. Secondly, based on the realistic CC/CV battery charging scheme rather than simple constant charging rate, IDCN considers not only undergoing queue and waiting queue of EVs for charging service but also reserving queue of EVs to calculate the waiting time, which is more precise compared to that of other algorithms. Thirdly, IDCN implements the global charging scheme by means of the minimum arrival time gap between the charging EV and its corresponding discharging EV, so the direct V2V charging efficiency is improved and then waiting time declines.

Besides, we explore the impacts of varying exchanged energy amount and charging information broadcast time interval T on waiting time of EVs in IDCN, and related results are shown in Fig. 13, where we set EV penetration ratio and stopping location number to 10% and 20, respectively. From this figure, it is easily observed that average waiting time is proportional to the exchanged energy amount of each EV, as more energy transaction requirements lead to higher charging time, which has significant influences on the increase of waiting time. In addition, Fig. 13 presents that when we raise the values of broadcast time interval, the average waiting time obtains distinct increase. The reasons are obvious: (1) higher T decreases the accuracy of busy situations of all stopping locations stored at the sides of MEC servers, and subsequently leads to inefficient local charging navigation, and (2) the rise of T imposes negative effects on the transmission of gathered local navigation decisions, which can affect the optimal performance of charging-discharging EV pair matching at the NCC side. As a result, the charging efficiency becomes lower and average waiting time rises.

TABLE 4. Total exchanged energy amount (value unit: KWh).

	PR_{ev}	IDCN	IDCN_S	DVCS	STCC	GCNA
$N_{sl}=10$	10%	798.5	720.0	535.1	508.9	423.2
	11%	805.0	727.0	572.7	554.3	473.2
	12%	827.3	754.2	596.8	574.2	496.1
	13%	842.0	770.6	610.3	589.0	503.8
	14%	851.2	787.3	629.2	590.1	520.3
	15%	886.5	793.2	640.1	603.7	524.5
	16%	906.2	828.9	646.0	634.8	529.3
	17%	927.6	866.4	667.8	637.8	554.0
	18%	1012.0	894.0	733.0	695.5	607.3
	19%	1040.8	900.2	768.7	721.2	633.5
	20%	1174.3	941.3	787.1	772.5	664.5
$N_{sl}=20$	10%	1222.1	1195.9	1120.0	1108.2	923.3
	11%	1357.8	1339.6	1180.4	1139.8	932.4
	12%	1490.2	1353.6	1240.9	1237.8	945.1
	13%	1623.8	1483.6	1282.6	1240.2	1020.3
	14%	1728.2	1552.9	1295.3	1265.7	1028.4
	15%	1774.3	1578.3	1358.9	1309.5	1047.0
	16%	1783.5	1586.0	1367.7	1329.1	1064.1
	17%	1798.7	1597.2	1373.5	1336.4	1086.0
	18%	1806.7	1647.1	1379.1	1344.0	1093.6
	19%	1901.5	1677.7	1380.0	1362.0	1116.2
	20%	1926.7	1794.9	1400.3	1375.1	1159.7

3) TOTAL EXCHANGED ENERGY AMOUNT AND CHARGED EV NUMBER

Table 4 and Fig. 14 indicate the total exchanged energy amount and the number of successfully charged EVs with varying EV penetration ratio PR_{ev} and stopping location number N_{sl}, respectively. First of all, we observe that when EV penetration ratio rises, more EVs can take part in the V2V charging services, as a result, both exchanged energy amount and charged EV number obtain obvious increase. Besides, both Table 4 and Fig. 14 present that the growth of stopping location number is beneficial to the increment of exchanged energy amount and charged EV number, because better candidate parking choice and more available stopping

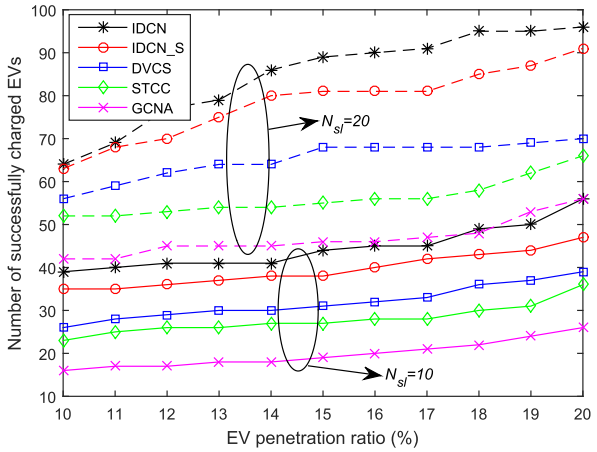

FIGURE 14. Successfully charged EV number with different EV penetration ratio and stopping location number.

slots are supplied to mobile EVs, and direct V2V charging efficiency can be significantly improved with the rise of stopping location number. Moreover, it is obvious that the performance of IDCN is best compared with that of other referencing charging navigation strategies, and there are some reasons to interpret such results as follows: (1) IDCN is capable of selecting the most available stopping location via considering charging comfortable degree with respect to more accurate waiting time and free parking slot ratio, which are very useful to alleviate the congestion status of stopping locations and mitigate the synchronous conflicts of stopping location selection for a large number of EVs, and (2) IDCN establishes an adequate global charging navigation scheme to realize the optimal charging-discharging EV pair matching, by means of arrival time interval and required energy gap between charging EVs and discharging EVs, and exchanged energy amount, all of which are beneficial to raising the EV pair matching number and achieving the maximum total exchanged energy. While IDCN_S makes use of static traffic information to compute EVs' arrival time in corresponding stopping locations, and does not take into account the reservation information of charging/discharging EVs to estimate the charging comfortable degree, as a result, the selected stopping location may suffer from congestions which lead to low V2V energy exchange efficiency. In STCC and GCNA, only required energy level (as long as the supplied energy is not less than the demanded energy) is considered in the process of charging-discharging EV pair matching, and essential temporal coordinations of EVs are neglected. In order to complete EV pair matching, DVCS considers the energy levels of charging-discharging EVs and FAFS (first arrive first service) principle, both of which are not enough to promise the efficient global EV pair assignments in a selected stopping location.

4) TIME COMPLEXITY

Based on various EV penetration ratio, Table 5 shows the time complexity of different matching methods (namely

TABLE 5. Time complexity evaluation (value unit: s).

PR_{ev}	KM-based algorithm	Permutation-based algorithm
10%	0.03	0.04
12%	0.14	0.75
14%	0.18	8.71
16%	0.26	113.58
18%	0.32	2.41e4
20%	0.56	3.82e5

KM-based algorithm and simple permutation-based algorithm) used in the proposed global charging navigation scheme, to obtain the optimal charging-discharging EV pair assignments. In this experiment, we set the number of stopping locations to 10. From table 5, we can observe that the two algorithms' calculation time increases with the rise of EV penetration ratio, which results in more EVs participating in V2V charging operations and heavier matching tasks in NCC side. In addition, this table presents that the calculation time of KM-based algorithm is far less than that of permutation-based algorithm, and the outcome can be explained from the perspective of theoretical analysis. In the KM-based algorithm, the size of matching is raised by 1 edge in each round and there are $O(n_{km})$ rounds to search the maximum matching (where $n_{km} = \max(|U|, |V|)$, U and V denote the charging EV set and discharging EV set, respectively), and in each round, total $O(n_{km}^2)$ is assigned to improve the labeling if no augmenting path is found, so the whole time complexity of KM-based algorithm is given as $O(n_{km}^3)$. While the time complexity of permutation-based algorithm is easily gained and it is expressed as $O(n_{pb})$, where $n_{pb} = \frac{n_1!}{(n_1-n_2)!}$, $n_1 = \max(|U|, |V|)$ and $n_2 = \min(|U|, |V|)$. In general, $||U| - |V||$ is small, and both $|U|$ as well as $|V|$ are large, so $O(n_{km}^3) \ll O(n_{pb})$.

V. CONCLUSION

In this paper, we have proposed an intelligent V2V charging navigation strategy for mobile EVs in VANET-based communication environments. Firstly, an efficient MEC-based semi-centralized charging navigation structure has been established to ensure the reliable charging information dissemination and feasible charging coordination with low cost of communication and calculation. After that, based on the derived charging factor models, namely, traveling time prediction model, charging time estimation model and charging comfortable degree model, we have designed an effective local charging navigation scheme and global charging navigation mechanism, to dynamically choose the optimal traveling route as well as stopping location for V2V charging operations, and achieve the best charging-discharging EV pair matching assignments, respectively. Finally, the simulation results and theoretical analyses have been given to demonstrate the effectiveness of our proposed strategy. In the future work, based on several factors including EV driver preferences, current calculation capacities of EVs and MEC servers, network communication quality and so on, we would

like to design an adaptive computation offloading adjustment scheme for mobile EVs, to dynamically assign charging navigation calculation tasks implemented by local execution on EVs, or full offloading on MEC servers, or partial offloading on MEC servers.

REFERENCES

[1] L. Li, S. Coskun, F. Zhang, R. Langari, and J. Xi, "Energy management of hybrid electric vehicle using vehicle lateral dynamic in velocity prediction," *IEEE Trans. Veh. Technol.*, vol. 68, no. 4, pp. 3279–3293, Apr. 2019.

[2] M. Ban, J. Yu, M. Shahidehpour, D. Guo, and Y. Yao, "Electric vehicle battery swapping-charging system in power generation scheduling for managing ambient air quality and human health conditions," *IEEE Trans. Smart Grid*, vol. 10, no. 6, pp. 6812–6825, Nov. 2019.

[3] Q. Wang, X. Liu, J. Du, and F. Kong, "Smart charging for electric vehicles: A survey from the algorithmic perspective," *IEEE Commun. Surveys Tuts.*, vol. 18, no. 2, pp. 1500–1517, 2nd Quart. 2016.

[4] E. S. Rigas, S. D. Ramchurn, and N. Bassiliades, "Managing electric vehicles in the smart grid using artificial intelligence: A survey," *IEEE Trans. Intell. Transp. Syst.*, vol. 16, no. 4, pp. 1619–1635, Aug. 2015.

[5] F. Xia, H. Chen, L. Chen, and X. Qin, "A hierarchical navigation strategy of EV fast charging based on dynamic scene," *IEEE Access*, vol. 7, pp. 29173–29184, 2019.

[6] S. Wang, S. Bi, Y.-J. A. Zhang, and J. Huang, "Electrical vehicle charging station profit maximization: Admission, pricing, and online scheduling," *IEEE Trans. Sustain. Energy*, vol. 9, no. 4, pp. 1722–1731, Oct. 2018.

[7] F. Wu and R. Sioshansi, "A two-stage stochastic optimization model for scheduling electric vehicle charging loads to relieve distribution-system constraints," *Transp. Res. B, Methodol.*, vol. 102, pp. 55–82, Aug. 2017.

[8] H. Qin and W. Zhang, "Charging scheduling with minimal waiting in a network of electric vehicles and charging stations," in *Proc. 8th ACM Int. Workshop Veh. Inter-Netw.*, Sep. 2011, pp. 51–60.

[9] Z. Moghaddam, I. Ahmad, D. Habibi, and Q. V. Phung, "Smart charging strategy for electric vehicle charging stations," *IEEE Trans. Transport. Electrific.*, vol. 4, no. 1, pp. 76–88, Mar. 2018.

[10] H. Yang, Y. Deng, J. Qiu, M. Li, M. Lai, and Z. Y. Dong, "Electric vehicle route selection and charging navigation strategy based on crowd sensing," *IEEE Trans. Ind. Informat.*, vol. 13, no. 5, pp. 2214–2226, Oct. 2017.

[11] Y. Cao, H. Song, O. Kaiwartya, B. Zhou, Y. Zhuang, Y. Cao, and X. Zhang, "Mobile edge computing for big-data-enabled electric vehicle charging," *IEEE Commun. Mag.*, vol. 56, no. 3, pp. 150–156, Mar. 2018.

[12] J. Liu, Y. Shi, Z. M. Fadlullah, and N. Kato, "Space-air-ground integrated network: A survey," *IEEE Commun. Surveys Tuts.*, vol. 20, no. 4, pp. 2714–2741, 4th Quart., 2018.

[13] N. Cheng, W. Xu, W. Shi, Y. Zhou, N. Lu, H. Zhou, and X. Shen, "Air-ground integrated mobile edge networks: Architecture, challenges, and opportunities," *IEEE Commun. Mag.*, vol. 56, no. 8, pp. 26–32, Aug. 2018.

[14] S. Dinkhah, C. A. Negri, M. He, and S. B. Bayne, "V2G for reliable microgrid operations: Voltage/frequency regulation with virtual inertia emulation," in *Proc. IEEE ITEC*, Detroit, MI, USA, Jun. 2019, pp. 1–6.

[15] H. Shareef, M. M. Islam, and A. Mohamed, "A review of the stage-of-the-art charging technologies, placement methodologies, and impacts of electric vehicles," *Renew. Sustain. Energy Rev.*, vol. 64, pp. 403–420, Oct. 2016.

[16] T. Sasaki, T. Kadoya, and K. Enomoto, "Study on load frequency control using redox flow batteries," *IEEE Trans. Power Syst.*, vol. 19, no. 1, pp. 660–667, Feb. 2004.

[17] M. Ehsani, M. Falahi, and S. Lotfifard, "Vehicle to grid services: Potential and applications," *Energies*, vol. 5, no. 10, pp. 4076–4090, Oct. 2012.

[18] B. Ramachandran, S. K. Srivastava, and D. A. Cartes, "Intelligent power management in micro grids with EV penetration," *Expert Syst. With Appl.*, vol. 40, no. 16, pp. 6631–6640, Nov. 2013.

[19] S. Huang and Q. Wu, "Dynamic tariff-subsidy method for PV and V2G congestion management in distribution networks," *IEEE Trans. Smart Grid*, vol. 10, no. 5, pp. 5851–5860, Sep. 2019.

[20] F. Erden, M. C. Kisacikoglu, and N. Erdogan, "Adaptive V2G peak shaving and smart charging control for grid integration of PEVs," *Electr. Power Compon. Syst.*, vol. 46, no. 13, pp. 1494–1508, Jan. 2019.

[21] T. J. C. Tiago, V. Monteiro, J. C. A. Fernandes, C. Couto, A. A. N. Meléndez, and J. L. Afonso, "New perspectives for vehicle-to-vehicle (V2V) power transfer," in *Proc. IEEE IECON*, Washington, DC, USA, Oct. 2018, pp. 5183–5188.

[22] P. You and Z. Yang, "Efficient optimal scheduling of charging station with multiple electric vehicles via V2V," in *Proc. IEEE Int. Conf. Smart Grid Commun. (SmartGridComm)*, Nov. 2014, pp. 716–721.

[23] R. Alvaro-Hermana, J. Fraile-Ardanuy, D. Janssens, L. Knapen, and P. J. Zufiria, "Peer to peer energy trading with electric vehicles," *IEEE Intell. Transp. Syst. Mag.*, vol. 8, no. 3, pp. 33–44, Jul. 2016.

[24] K. Zhang, Y. Mao, S. Leng, S. Maharjan, Y. Zhang, A. Vinel, and M. Jonsson, "Incentive-driven energy trading in the smart grid," *IEEE Access*, vol. 4, pp. 1243–1257, Apr. 2016.

[25] P. You, Z. Yang, M.-Y. Chow, and Y. Sun, "Optimal cooperative charging strategy for a smart charging station of electric vehicles," *IEEE Trans. Power Syst.*, vol. 31, no. 4, pp. 2946–2956, Jul. 2016.

[26] C. D. Cauwer, W. Verbeke, J. Van Mierlo, and T. Coosemans, "A model for range estimation and energy-efficient routing of electric vehicles in real-world conditions," *IEEE Trans. Intell. Transp. Syst.*, to be published.

[27] M. Wang, M. Ismail, R. Zhang, X. Shen, E. Serpedin, and K. Qaraqe, "Spatio-temporal coordinated V2V energy swapping strategy for mobile PEVs," *IEEE Trans. Smart Grid*, vol. 9, no. 3, pp. 1566–1579, May 2018.

[28] C. P. Dubey, V. Kumar, B. Sharma, and G. Kaur, "Shortest path algorithm for distributed VANET using grid computing," in *Proc. IEEE ICSSIT*, Tirunelveli, India, Dec. 2018, pp. 118–121.

[29] A.-M. Koufakis, E. S. Rigas, N. Bassiliades, and S. D. Ramchurn, "Offline and online electric vehicle charging scheduling with V2V energy transfer," *IEEE Trans. Intell. Transp. Syst.*, to be published.

[30] G. Li, L. Boukhatem, L. Zhao, and J. Wu, "Direct vehicle-to-vehicle charging strategy in vehicular Ad-Hoc networks," in *Proc. IEEE NTMS*, Paris, France, Feb. 2018, pp. 1–5.

[31] G. Li, L. Boukhatem, and S. Martin, "An intersection-based QoS routing in vehicular ad hoc networks," *Mobile Netw. Appl.*, vol. 20, no. 2, pp. 268–284, Apr. 2015.

[32] G. Li, L. Boukhatem, and J. Wu, "Adaptive quality-of-service-based routing for vehicular ad hoc networks with ant colony optimization," *IEEE Trans. Veh. Technol.*, vol. 66, no. 4, pp. 3249–3264, Apr. 2017.

[33] W. Tong, A. Hussain, W. X. Bo, and S. Maharjan, "Artificial intelligence for vehicle-to-everything: A survey," *IEEE Access*, vol. 7, pp. 10823–10843, 2019.

[34] H. Khelifi, S. Luo, B. Nour, A. Sellami, H. Moungla, and F. Naït-Abdesselam, "An optimized proactive caching scheme based on mobility prediction for vehicular networks," in *Proc. IEEE GLOBECOM*, Abu Dhabi, United Arab Emirates, Dec. 2018, pp. 1–6.

[35] C. F. Daganzo, "The cell transmission model: A dynamic representation of highway traffic consistent with the hydrodynamic theory," *Transp. Res. Part B, Methodol.*, vol. 28, no. 4, pp. 269–287, Aug. 1994.

[36] Q. Mao, F. Hu, and Q. Hao, "Deep learning for intelligent wireless networks: A comprehensive survey," *IEEE Commun. Surveys Tuts.*, vol. 20, no. 4, pp. 2595–2621, 4th Quart. 2018.

[37] Z. Gao, D. Chen, P. Sun, and S. Cai, "KM-based efficient algorithms for optimal packet scheduling problem in celluar/infostation integrated networks," *Ad Hoc Netw.*, vol. 77, pp. 84–94, Aug. 2018.

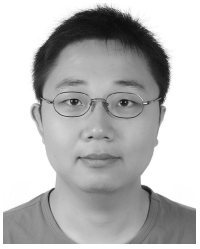

GUANGYU LI received the B.S. degree from the China University of Mining and Technology and the M.S. degree from Tongji University, China, in 2008 and 2011, respectively, and the Ph.D. degree from the University of Paris-Sud, Paris, France, in 2015. He is currently an Assistant Professor with the Key Laboratory of Intelligent Perception and Systems for High-Dimensional Information of Ministry of Education, Nanjing University of Science and Technology, Nanjing, China. His research interests include information dissemination in vehicle networks, big data mining, electric vehicles charging/discharging scheduling strategy, and traffic control.

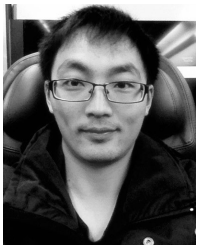

QIANG SUN received the B.S. degree from Hubei University and the M.S. degree from Shanghai University, China, in 2009 and 2012, respectively, and the Ph.D. degree from the University of Paris-Saclay, Paris, France, in 2016. He is currently an Assistant Professor with the School of Mathematical Science, Yangzhou University, Yangzhou, China. His research interests include graph coloring, graph homomorphism, Hamiltonian problems, and algorithms on graphs.

LILA BOUKHATEM received the degree in computer science engineering from the INI Institute, in 1997, the M.Sc. degree from the University of Versailles Saint Quentin-en-Yvelines, in 1998, and the Ph.D. degree from the University of Pierre et Marie Curie (Paris 6), in 2001. She is currently an Associate Professor with the ROCS (Networks and combinatorial and stochastic optimization) Team, LRI Laboratory, University of Paris-Sud 11. She joined the LRI Laboratory, in 2002, where she is developing various research works in mobile and wireless networks, including cross-layer design, modeling and performance evaluation, radio resource allocation and optimization (TDMA and OFDMA systems), mobility management, and routing and energy in ad hoc networks. She has lead and actively participated to several national and international projects and programs, such as PHC Sakura, FP7-NoE NEWCOM, and EIT ICT-Labs Digital Cities. Her current research interests include routing in vehicular networks and interference mitigation in OFMDA systems.

JINSONG WU (SM'11) received the Ph.D. degree from the Department of Electrical and Computer Engineering, Queen University, Canada. He received the 2017 and 2019 IEEE System Journal Best Paper Awards. His coauthored article received the 2018 IEEE TCGCC Best Magazine Paper Award. He received the IEEE Green Communications and Computing Technical Committee 2017 Excellent Services Award for Excellent Technical Leadership and Services in the Green Communications and Computing Community. He was the leading Editor and coauthor of the comprehensive book, entitled *Green Communications: Theoretical Fundamentals, Algorithms, and Applications* (CRC Press, 2012). He is an elected Vice-Chair of Technical Activities of the IEEE Environmental Engineering Initiative, a pan-IEEE effort under the IEEE Technical Activities Board (TAB). He was the Founder and Founding Chair of the IEEE Technical Committee on Green Communications and Computing (TCGCC). He is also the Co-Founder and Founding Vice-Chair of the IEEE Technical Committee on Big Data (TCBD).

JIAN YANG received the Ph.D. degree in pattern recognition and intelligence systems from the Nanjing University of Science and Technology (NUST), in 2002. In 2003, he was a Postdoctoral Researcher with the University of Zaragoza. From 2004 to 2006, he was a Postdoctoral Fellow with the Biometrics Centre, Hong Kong Polytechnic University. From 2006 to 2007, he was a Postdoctoral Fellow with the Department of Computer Science, New Jersey Institute of Technology. He is currently a Chang-Jiang Professor with the School of Computer Science and Technology, NUST. His academic publications have been cited more than 4000 times in the ISI Web of Science, and 16000 times in the Web of Scholar Google. His research interests include pattern recognition, computer vision, machine learning, and intelligent transportation. He is an IAPR Fellow.